



# Two extreme contact binary systems in the nearest globular cluster M4

L. Liu,<sup>1,2,3,4</sup>★ S.-B. Qian<sup>1,2,3,4</sup> and E. Fernández-Lajús<sup>5</sup>

<sup>1</sup>National Astronomical Observatories/Yunnan Observatory, Chinese Academy of Sciences, P O Box 110, 650011 Kunming, China

<sup>2</sup>Key Laboratory for the Structure and Evolution of Celestial Objects, Chinese Academy of Sciences, 650011 Kunming, China

<sup>3</sup>United Laboratory of Optical Astronomy, Chinese Academy of Sciences (ULOAC), 100012 Beijing, China

<sup>4</sup>Graduate School of the CAS, Yuquan Road 19, Shijingshan Block, 100049 Beijing, China

<sup>5</sup>Facultad de Ciencias Astronómicas y Geofísicas, Universidad Nacional de La Plata and Instituto de Astrofísica de La Plata (CCT La Plata – CONICET/UNLP), Paseo del Bosque s/n, 1900 La Plata, Argentina

Accepted 2011 March 25. Received 2011 March 24; in original form 2010 July 22

## ABSTRACT

We present the results of photometric solutions for two contact binaries in the nearby globular cluster M4. We estimate their physical parameters using the light-curve program of the Wilson–Devinney code. These systems have quite different mass ratios, which indicates that they did not form at the same time. V47 is an extreme mass-ratio system ( $q = 0.123 \pm 0.002$ ) being dissimilar to the same kind of field contact binaries. V53 is a high mass-ratio ( $q = 1.230 \pm 0.004$ ), deep-contact ( $f = 79.7 \pm 1.9$  per cent) system. It is also a blue straggler.

**Key words:** binaries: eclipsing – blue stragglers – stars: evolution – stars: individual: V47 – stars: individual: V53.

## 1 INTRODUCTION

Once, people believed that there were no binaries in globular clusters (GCs). However, this thought has been changed by new discoveries in the last 20 yr. Many binaries have been discovered in GCs, including numbers of contact binaries. Binary populations in GCs, especially primordial close binaries, play a very important role in the dynamical evolution of GCs. Consider a typical GC with a mass of  $M = 10^5 M_\odot$  and a root-mean-square velocity of  $\langle v^2 \rangle^{1/2} = 10 \text{ km s}^{-1}$ . According to the virial theorem, the binding energy of the GC is  $E = -M\langle v^2 \rangle/2 = -1 \times 10^{43} \text{ J}$ . If a binary is made up of two  $1 M_\odot$  stars with a separation of  $2 R_\odot$ , its binding energy is  $1 \times 10^{41} \text{ J}$ . The total binding energy contained in 100 such binaries can compare with that of the whole GC. If these binary systems exchange energy with passing stars, the structure and evolution of a GC should be strongly affected.

Binaries in GCs not only impact the dynamical evolution of GCs but also are windows to understand the absolute dimensions of GC stars. As early as 1983, Harris & McClure (1983) pointed out that the GC giants had lower masses and larger radii than field Population I giants. A deduction is that field main-sequence stars (MSs) and GC MSs should be somewhat different. Contact binaries are potentially a powerful tool to understand the parameters of GC MSs, because they are usually made up of two MSs. This is the aim of this paper.

Kaluzny, Rucinski, Mateo and other researchers have studied GC contact binaries extensively. Through 2000, the number of contact binaries discovered in and around GCs was 86 (Rucinski 2000). Except for a W UMa contact binary in the GC NGC 6397 which was studied by Rubenstein & Bailyn (1996), none of these has published physical parameters. This paper gives parameters for two

GC contact binaries determined from their multicolour light curves. Because of the lack of spectroscopic data, these results should be considered preliminary.

## 2 OBSERVATIONS AND DATA ANALYSIS

The observations of the M4 field in  $B$ ,  $V$ ,  $R$  and  $I$  bands were carried out on 2010 June, 5, 6, 7 and 8 with the 2.15 m Jorge Sahade (JS) reflecting telescope (f/8.5 Cassegrain) at Complejo Astronómico El Leoncito Observatory (CASLEO), San Juan, Argentina. The nights were very clear with seeing of  $\sim 2.5$ – $3.0$  arcsec. The Versarray 1300B CCD camera was binned  $3 \times 3$ , yielding a scale of 0.67 arcsec per binned pixel and a field of view of  $5 \times 5 \text{ arcmin}^2$ . Exposure times were 120 s for  $B$  and 90 s for  $VRI$ . The comparison star is marked as C1 in Fig. 1, whose brightness is close to our targets. The point spread function (PSF) method is used to reduce the observed images with IRAF.<sup>1</sup> A PSF was derived for every image and used to measure the photometric magnitudes of the targets. The original measurements with the PSF method are listed in Appendix A (Tables A1–A7). The photometric uncertainties in these tables are those produced by the IRAF program. They depend on, as is well known, the correct input parameters, such as the full width at half-maximum PSF, the standard deviation of the background in counts, the readout noise etc. They also depend on the quality of the PSF fit. For these observations, the photometric uncertainties are about 0.04 mag. Because V53 is located in a very crowded field of the cluster, the value of the standard deviation of the background is easily overestimated, which will lead to a large uncertainty. Thus, the

<sup>1</sup> IRAF is distributed by the National Optical Astronomy Observatories, which are operated by the Association of Universities for Research in Astronomy, Inc., under cooperative agreement with the National Science Foundation.

\*E-mail: creator\_ll.student@sina.com; liul@ynao.ac.cn

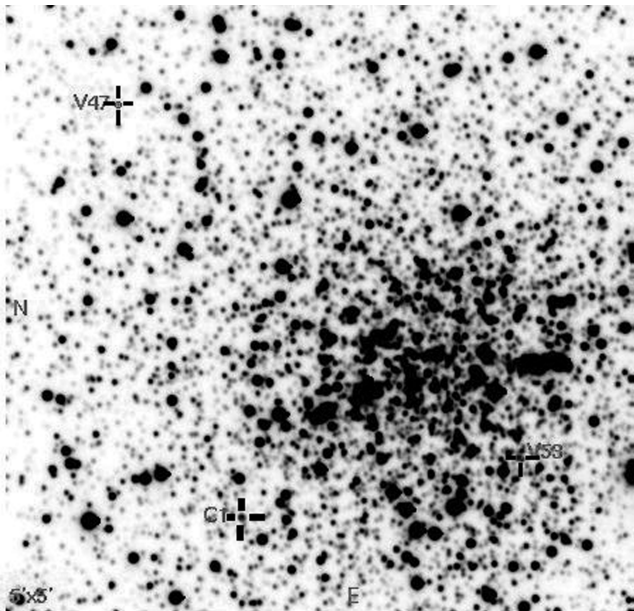


**Figure 1.** CCD photograph of nearby GC M4. The contact binaries V47 and V53 are marked in the picture. C1 is the comparison star.

**Table 1.** Times of minima of V47 and V53 in M4.

Star	JD (Hel.)	Error (d)	Filters	Ref. <sup>a</sup>
V47	244 9869.53640	0.0001		(1)
	245 5352.69351	0.00021	R	(2)
	245 5352.69450	0.00109	I	(2)
	245 5352.82929	0.00099	R	(2)
	245 5353.63854	0.00039	I	(2)
	245 5353.77418	0.00023	R	(2)
	245 5353.77428	0.0004	I	(2)
	245 5354.58349	0.00048	V	(2)
	245 5354.71913	0.00048	V	(2)
	245 5355.52718	0.0004	B	(2)
	245 5355.66298	0.00048	B	(2)
	244 9869.53640	0.0001		(1)
	245 5352.72445	0.00060	R	(2)
V53	245 5353.64981	0.00069	I	(2)
	245 5354.57463	0.00059	V	(2)
	245 5354.73894	0.00098	V	(2)
	245 5355.65446	0.00064	B	(2)

<sup>a</sup>(1) – Kaluzny et al. (1997); (2) – this paper.

uncertainties for V53 were possibly overestimated. For this reason, we did not use the uncertainties in the Wilson–Devinney (w–d) code when fitting the light curves of V53. The uncertainties are shown in Fig. 3 for the purpose of describing the quality of our photometric measurements.

We use the least-squares parabolic fitting method to get several times of minima through our observations and collected all available times of minima of V47 and V53 for their ephemeris correction, which are listed in Table 1. The corrected ephemerides are

$$245\ 5352.6938(\pm 0.0002) + 0.269\ 973\ 29(\pm 0.000\ 000\ 03) E \quad (1)$$

and

$$245\ 5355.6568(\pm 0.0019) + 0.308\ 5123(\pm 0.000\ 0003) E. \quad (2)$$

We use these formulas to calculate the phases, finding that the light curves of V53 are a bit incomplete and noisy because this star is

mixed with other sources in the crowded field and so is very sensitive to seeing changes. There is an obvious distortion in the *B*-band data for V47, which is not detected in the other bands.

### 3 PHOTOMETRIC SOLUTIONS

Because the stars are faint, there are no previous spectral measurements or photometric solutions of these two systems. We give their photometric parameters first. Having considered the qualities of the light curves, we choose the *VRI* light curves of V47 and the *BRI* light curves of V53 for photometric analysis. The 2003 version of the w–d program (Wilson & Devinney 1971; Wilson 1990, 1994; Wilson & Van Hamme 2003) is used to fit the light curves. During the solutions, the effective temperature of star 1,  $T_1$ , is fixed at values described below. Also fixed at values chosen from the literature are the bolometric albedos,  $A_1$  and  $A_2$ , the gravity-darkening coefficients,  $g_1$  and  $g_2$ , and the limb-darkening coefficients of each band. The quantities varied in the fit are the mass ratio,  $q$ , the effective temperature of star 2,  $T_2$ , the monochromatic luminosity of star 1 in each band,  $L_1$ , the orbital inclination,  $i$ , and the dimensionless potential of star 1,  $\Omega_1$ . Extensive testing revealed that these two systems are contact systems, so the contact model is used in the final solutions (Mode 3,  $\Omega_1 = \Omega_2$ ). These inputs and outputs are listed in Table 2.

#### 3.1 V47

Kaluzny, Thompson & Krzeminski (1997) gave  $(B - V)_{\max}$  as 0.82 for V47 and the reddening  $E(B - V)$  as 0.4 for M4. However, the latest reddening value was given by Richer et al. (2004) as  $E(B - V) = A_V/R_V = 1.33/3.8 = 0.35$ . So  $(B - V)_0 = 0.47$  for V47 if it is a member of M4. An  $[Fe/H] = -1.2$ ,  $[\alpha/Fe] = 0.2$ , age = 2.0 Gyr (parameters of M4; Richer et al. 2004) isochrone from the Dartmouth Stellar Evolution Database (Dotter et al. 2007, 2008; <http://stellar.dartmouth.edu/models/>) has  $T_{\text{eff}} = 6238$  K at  $(B - V)_0 = 0.47$ . Indeed, the value of the effective temperature sensitively depends on the uncertainties of the previous parameters. It is hard to exactly determine the effective temperature without any spectral data. Fortunately, the light curve depends much more sensitively on the ratio of the two  $T_{\text{eff}}$  values than on the individual  $T_{\text{eff}}$  values (Yakut & Eggleton 2005). Thus, the derived values of the other parameters of the systems such as mass ratio, inclination and degree of contact are probably not much affected by the uncertainties in the  $T_{\text{eff}}$ . Hence, for an estimation,  $T_1$  is fixed at 6238 K. Evolution theory of single stars tells us that low-mass MSs have a radiative core with a convective envelope; contrarily, medium-mass stars have a convective core with a radiative envelope. We adopt the first case, so the bolometric albedos are  $A_1 = A_2 = 0.5$  for the convective-equilibrium envelope (Rucinski 1969). The values of the gravity-darkening coefficient  $g_1 = g_2 = 0.32$  (Lucy 1967) are used, which correspond to the common convective envelope of both components. According to Claret & Giménez (1990), square-root limb-darkening coefficients are used for each band (listed in Table 2). The main photometric results are  $q = 0.123 \pm 0.002$ ,  $T_2 = 6244 \pm 21$  K and  $f = 32.0 \pm 7.3$  per cent. These indicate that V47 is an extreme mass-ratio, medium-contact binary. The measurements, the observational errors and the fitted light curves are shown in Fig. 2.

**Table 2.** Photometric solutions for V47 and V53 in M4.

Parameters	Photometric elements		Errors	Photometric elements		Errors
	V47	V53		V47	V53	
$g_1 = g_2$	0.32	Assumed	0.32	Assumed		
$A_1 = A_2$	0.50	Assumed	1.00	Assumed		
$x_{1\text{bolo}} = x_{2\text{bolo}}$	0.145	Assumed	0.072	Assumed		
$y_{1\text{bolo}} = y_{2\text{bolo}}$	0.576	Assumed	0.660	Assumed		
$x_{1B} = x_{2B}$	–	Assumed	0.070	Assumed		
$y_{1B} = y_{2B}$	–	Assumed	0.811	Assumed		
$x_{1V} = x_{2V}$	0.146	Assumed	–	Assumed		
$y_{1V} = y_{2V}$	0.671	Assumed	–	Assumed		
$x_{1R} = x_{2R}$	0.039	Assumed	–0.075	Assumed		
$y_{1R} = y_{2R}$	0.688	Assumed	0.748	Assumed		
$x_{1I} = x_{2I}$	–0.025	Assumed	–0.124	Assumed		
$y_{1I} = y_{2I}$	0.656	Assumed	0.694	Assumed		
$T_1$	6238 K	Assumed	7350 K	Assumed		
Period shift	–	–	0.0504	$\pm 0.0008$		
$q$	0.123	$\pm 0.002$	1.230	$\pm 0.004$		
$\Omega_{\text{in}}$	2.0275	Assumed	4.1149	Assumed		
$\Omega_{\text{out}}$	1.9476	Assumed	3.5533	Assumed		
$T_2$	6244 K	$\pm 21$ K	7523 K	$\pm 40$ K		
$i$	72°149	$\pm 0.4$	39°691	$\pm 0.2$		
$L_1/(L_1 + L_2)(B)$	–	–	0.4283	$\pm 0.0064$		
$L_1/(L_1 + L_2)(V)$	0.8618	$\pm 0.0031$	–	–		
$L_1/(L_1 + L_2)(R)$	0.8620	$\pm 0.0029$	0.4415	$\pm 0.0038$		
$L_1/(L_1 + L_2)(I)$	0.8622	$\pm 0.0027$	0.4469	$\pm 0.0028$		
$\Omega_1 = \Omega_2$	2.0019	$\pm 0.0058$	3.6675	$\pm 0.0106$		
$r_1(\text{pole})$	0.5283	$\pm 0.0017$	0.3962	$\pm 0.0017$		
$r_1(\text{side})$	0.5877	$\pm 0.0027$	0.4288	$\pm 0.0023$		
$r_1(\text{back})$	0.6092	$\pm 0.0033$	0.5233	$\pm 0.0065$		
$r_2(\text{pole})$	0.2110	$\pm 0.0054$	0.4295	$\pm 0.0016$		
$r_2(\text{side})$	0.2204	$\pm 0.0066$	0.4671	$\pm 0.0022$		
$r_2(\text{back})$	0.2624	$\pm 0.0158$	0.5441	$\pm 0.0048$		
$f$	32.0 per cent	$\pm 7.3$ per cent	79.7 per cent	$\pm 1.9$ per cent		

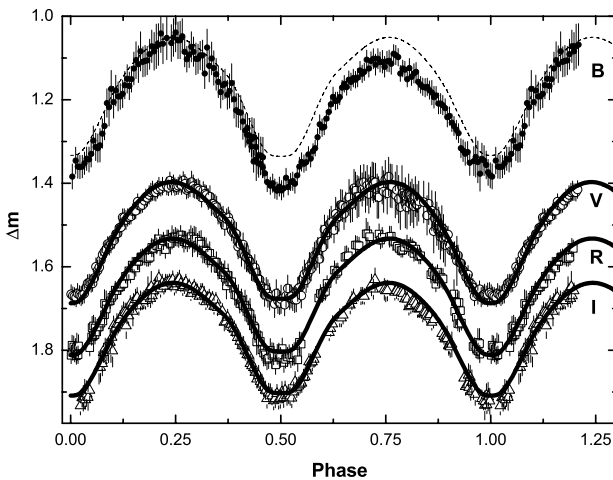


**Figure 2.** Observed (symbols) and theoretical (solid lines) light curves in the VRI bands for V47 under the condition  $A_1 = A_2 = 0.5$ . Error bars give the uncertainty of each measurement. The dashed line is a comparison with the  $B$ -band data. Because of the big distortion, the data in the  $B$  band are not used in the photometric solution.

### 3.2 V53

Kaluzny et al. (1997) gave  $(B - V)_{\text{max}}$  as 0.59 for V53. Like V47, assuming that V53 is a member of M4 yields  $(B - V)_0 = 0.24$ .

Its spectral type should be A7-8V. Using the same method as for V47, the corresponding temperature is 7535 K. However, recently, Lovisi et al. (2010) derived its temperature as 7350 K from a spectrum by using the Very Large Telescope (VLT). So we adopted the later value in the solution. The bolometric albedos are  $A_1 = A_2 = 1.0$  for a radiative equilibrium envelope; the values of the gravity-darkening coefficient are  $g_1 = g_2 = 0.32$ . Square-root limb-darkening coefficients are used for the  $BRI$  band (they are listed in Table 2). The main photometric results are  $q = 1.230 \pm 0.004$ ,  $T_2 = 7523 \pm 40$  K and  $f = 79.7 \pm 1.9$  per cent. V53 is a high mass-ratio, deep-contact, A-type contact binary. The measurements, the observational errors and the fitted light curves are shown in Fig. 3.

## 4 DETERMINATION OF PHYSICAL PARAMETERS

Based on the apparent distance modulus in the  $V$  band of M4,  $(m - M)_V = 12.83$  (Gratton et al. 2010), we compute the physical parameters of the two targets. The details are as follows.

First, we calculate the  $V$ -band absolute magnitude of the systems by  $M_{v_{\text{max}}} = m_{v_{\text{max}}} - \text{apparent distance modulus}$ . The maximum magnitude  $m_{v_{\text{max}}}$  appears at phase 0.25 or phase 0.75, when both surfaces of the two components face us. Each component contributes its luminosity to the  $M_{v_{\text{max}}}$ . Then, having considered bolometric corrections of F7V- and A8V-type MSs in the  $V$  band ( $-0.19$  mag for V47 and  $-0.09$  mag for V53; Schmidt-Kaler 1982), we obtain

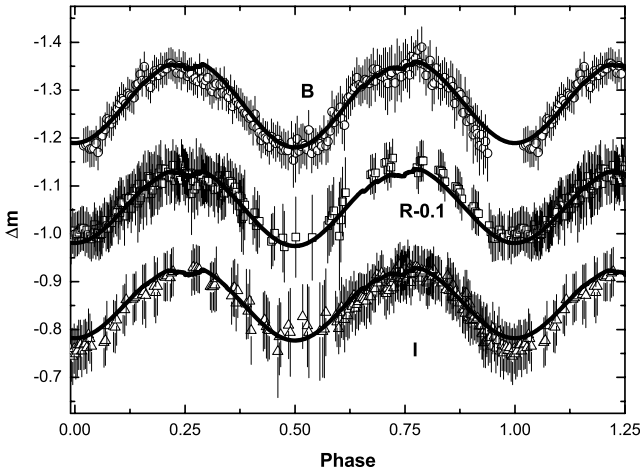


**Figure 3.** Observed and theoretical light curves in *BRI* bands for V53. The symbols have the same meaning as in Fig. 2.

bolometric absolute magnitudes,  $M_{\text{bol}}$ , for the systems (3.83 mag for V47 and 2.83 mag for V53). Secondly, we use the light curve (LC) program of the w–d code to estimate the combined bolometric absolute magnitudes which can be compared with the results in the previous step. The LC program can provide  $M_{\text{bol}}$  of each component from the period, semimajor axis and other parameters obtained from the photometric solutions. There is only one variable here, namely, the semimajor axis. Take V47 for an example. Every value of the semimajor axis corresponds a set of bolometric absolute magnitudes of star 1 and star 2. We add them to get the total value and find that when the semimajor axis is  $2.160 R_{\odot}$ , the bolometric absolute magnitudes of star 1 and star 2 are 3.99 and 5.95 mag, respectively, yielding  $M_{\text{bol,max}} = 3.826$  mag. This agrees with the observed value within the round-off errors. These inputs yield a set of physical parameters of V47, which are listed in Table 3. The parameters of V53 obtained in the same way are listed in Table 3 as well. We note that the total mass of V53 is about  $1.65 M_{\odot}$ . This value is twice the mass of the stars at the main-sequence turn-off ( $M_{\text{TO}} = 0.815 M_{\odot}$ ; Gratton et al. 2010), which is in accord with the conclusion that V53 is blue straggler. This reliable result is contributed by the effective temperature of V53 derived from the VLT spectrum.

## 5 DISCUSSION AND CONCLUSIONS

V47 and V53 are contact binaries that are members of the old, nearest GC M4. However, they are quite different. This at least implies that the two systems did not form at the same time. Usually, a close system evolves towards lower energy and angular momentum. So, contact binaries must evolve from high mass ratio to low mass ratio to decrease its total energy and angular momentum. Its larger  $q$  argues that V53 has been in contact for less time than V47. However, there are two doubts. First, the photometric solution reveals that V53 has a very low orbital inclination and a deep contact factor. This kind of system, with such a low orbital inclination and with such a deep contact factor but a mass ratio close to one, is very

rare. Secondly, V53 is a blue straggler (BS). BSs are above the turn-off point in the cluster colour–magnitude diagram. They seem very young, blue and bright. Since the 1990s, several observations imply that their formation is related to binaries. (a) Some BSs are short-period binary systems, like V53. (b) The spatial distribution of BSs and binaries is similar (Mathieu & Latham 1986; Nemec & Harris 1987; Nemec & Cohen 1989). These observations led to the interpretation that BSs come from mass transfer between the components of close binaries or come from the merging of close binaries by orbital angular momentum loss. The photometric results show that the components of V53 are still located on the main sequence because of their surface gravity  $g$ . However, their luminosities are large than expected for their masses. A rational explanation is that, when V53 merged, lots of heat was generated and has not dissipated completely yet. This process left a high-temperature, low-mass abnormal system. It can be proved by long-term monitoring, since the brightness should decrease due to the heat radiating away. Existing circumstantial evidence for this picture is provided by the amplitude of the light variation. We checked the light curve published by Kaluzny et al. (1997), finding  $\text{MaxII} - \text{MinII} \sim 0.22$  mag. In our light curves, this value has decreased to  $\sim 0.20$  mag, on average. This can be explained as follows. As the merging process continues, the shape of the system will change from asymmetric to symmetric and the variations caused by the geometric shape will eventually disappear. Hence, V53 is very worthwhile paying attention to.

Let us move our sight to the other target, V47. We define an extreme mass-ratio, deep-contact binary system (EMRDCBS) as a W UMa-type binary whose mass ratio is less than 0.20 and whose fill-out factor is greater than 50 per cent. Generally, they are at the last stage of contact binary evolution. Perhaps they are already rapidly rotating single stars. This type of binary is thought to end its evolution by merging into a single star in two different ways. In one case, when the mass transfer is from the less massive secondary component to the more massive primary, the period of the system is increasing with the mass ratio decreasing. If the orbital angular momentum is less than three times the total spin angular momentum, the system will become unstable and evolve into a single, rapidly rotating star (Hut 1980). In the other case, when the mass transfer is from the more massive primary component to the less massive secondary, maybe with lots of mass lost from the second Lagrange point ( $L_2$ ), the orbit of the system is contracting with the mass ratio decreasing. The evolution ends with the small star being consumed by the big star (Rasio & Shapiro 1995).

V47 is such a system: it has a low mass ratio ( $\sim 0.123$ ) and medium contact ( $\sim 32$  per cent). Its period is shorter than and the mass of its secondary is among the smallest of those known for EMRDCBSs (Table 4). There are two possible reasons for these properties of V47. First, interactions of third stars with short-period binaries in GCs are expected to reduce the orbital separation, on average (e.g. see the discussion in section 3.2 of Hut et al. 1992). Decreasing the orbital separation would increase the depth of the contact. Secondly, MSs in GCs have lower masses than those in the typical field contact binary. The period–luminosity relation for contact binaries then argues that the cluster binaries will have shorter

**Table 3.** Physical parameters of V47 and V53.

	$M_1 (M_{\odot})$	$M_2 (M_{\odot})$	$R_1 (R_{\odot})$	$R_2 (R_{\odot})$	$A (R_{\odot})$	$\log g_1 (\text{cgs})$	$\log g_2 (\text{cgs})$	$M_{\text{bol}1}$	$M_{\text{bol}2}$	$M_{\text{bol}}$	$m_{\text{lmax}}$
V47	1.66	0.20	1.24	0.50	2.160	4.47	4.35	3.99	5.95	3.826	16.85
V53	0.74	0.91	1.01	1.08	2.270	4.30	4.33	3.73	3.46	2.830	15.75

**Table 4.** Physical parameters of some deep, extreme mass-ratio field contact binaries.

Name	$P$ (d)	$q$	$M_1$ ( $M_\odot$ )	$M_2$ ( $M_\odot$ )	$R_1$ ( $R_\odot$ )	$R_2$ ( $R_\odot$ )	$L_1$ ( $L_\odot$ )	$L_2$ ( $L_\odot$ )	$f$ (per cent)	References
AH Aur	0.4941	0.167	1.68	0.28	1.87	0.90	4.57	1.22	75.0	Gazeas et al. (2005)
V410 Aur	0.3664	0.146	1.30	0.19	1.40	0.61	2.31	0.41	52.4	Yang, Qian & Zhu (2005)
CK Boo	0.3552	0.112	1.43	0.16	1.44	0.56	2.72	0.43	65.0	Kalci & Derman (2005)
V345 Gem	0.2748	0.143	1.05	0.15	1.09	0.49	1.75	0.30	72.9	Yang et al. (2009)
YY CrB	0.3766	0.245	1.43	0.35	1.43	0.81	2.56	0.82	63.4	Gazeas et al. (2005)
FG Hya	0.3278	0.110	1.45	0.16	1.40	0.58	2.11	0.39	85.6	Qian & Yang (2005)
TV Mus	0.4457	0.163	1.29	0.21	1.60	0.78	2.88	0.62	74.3	Qian et al. (2005)
V2388 Oph	0.8023	0.188	1.76	0.33	2.58	1.29	13.34	2.64	65.0	Yakut, Kalomeni & Ibanoglu (2004)
DZ Psc	0.3661	0.142	1.34	0.19	4.44	0.66	2.72	0.60	79.0	Gazeas et al. (2005)
Y Sex	0.4198	0.177	0.62	0.11	1.19	0.60	1.87	0.44	64.0	Yang & Liu (2003)
HV UMa	0.7108	0.190	2.84	0.54	2.62	1.18	17.22	2.95	61.9	Csak et al. (2000)
GR Vir	0.3278	0.115	1.30	0.15	1.34	0.57	2.48	0.41	78.6	Lu & Rucinski (1999)

periods. In addition, Rubenstein (2001) and others have pointed out that Population II MSs have smaller masses and radii at a given colour than Population I stars. Contact binaries made of Population II stars will have smaller separations, hence shorter orbital periods, than those made of Population I stars with the same mass. In addition to its short period, the fill-out factor of V47 is remarkable. Ordinarily, low mass-ratio systems should have a deep contact configuration (Table 4). However, V47 is far away from this expected state. This may reflect the process that the mass is transferring from the less massive component to the more massive one, which causes the orbit to enlarge. This causes the system to exhibit a low mass ratio but a medium contact factor. Because of interactions with third stars, this mass-transfer process might be stronger in clusters than that in the field. This idea can be tested by long-term monitoring of the times of minimum. Unlike V53, the observation of V47 is much easier.

In summary, (a) V47 and V53 both are short-period, small-amplitude contact binaries in the old GC M4. The distinctions are that V47 has an extreme mass ratio and medium fill-out factor, while V53 has a high mass ratio and deep fill-out factor. (b) V47 presents some different properties from field low mass-ratio contact binaries. These differences may be a window on the dynamical impact of GCs on their binary stars. (c) V53 is not only a contact binary but also a BS. This dual nature makes it an important object to comprehend the hypothesis that BSs are formed by binaries.

It must be pointed out that, because of the seeing, the photometric measurements were of poorer quality than is desirable. Moreover, because of the small orbital inclinations, the mass ratio,  $q$ , may perhaps be less reliable, with radial velocity measurement becoming very important. In the future, we will apply to obtain radial velocities with a 6–8 m telescope in order to determine spectroscopic mass ratios and much more exact parameters. This will provide the evidence needed to support our conclusions.

## ACKNOWLEDGMENTS

This work is partly supported by Chinese Natural Science Foundation (No. 10878012, No. 10973037 and No. 10903026), the National Key Fundamental Research Project through grant 2007CB815406, the Yunnan Natural Science Foundation (No. 2008CD157) and by West Light Foundation of the Chinese Academy of Sciences. New observations of the system were obtained with the 2.15-m telescope at CASLEO, San Juan, Argentina. We highly appreciate the all helps afforded by the referee. These helps improved the paper greatly.

## REFERENCES

- Csak B., Kiss L. L., Vinko J., Alfaro E. J., 2000, A&A, 356  
 Claret A., Gimenez A., 1990, A&A, 230, 412  
 Dotter A., Chaboyer B., Jevremovic D., Baron E., Ferguson J. W., Sarajedini A., Anderson J., 2007, AJ, 134, 376  
 Dotter A., Chaboyer B., Jevremovic D., Kostov V., Baron E., Ferguson J. W., 2008, ApJS, 178, 89  
 Gazeas K. D. et al., 2005, Acta Astron., 55, 123  
 Gratton R. G., Carretta E., Bragaglia A., Lucatello S., S’Orazi V., 2010, A&A, 517, A81  
 Harris H. C., McClure R. D., 1983, ApJ, 265, L77  
 Hut P., 1980, A&A, 92, 167  
 Hut P. et al., 1992, PASP, 104, 981  
 Kalci R., Derman E., 2005, Astron. Nachr., 326, 342  
 Kaluzny J., Thompson I. B., Krzeminski W., 1997, AJ, 113, 2219  
 Lovis L. et al., 2010, ApJ, 719, L121  
 Lu W.-X., Rucinski S. M., 1999, AJ, 118, 515  
 Lucy L. B., 1967, Z. Astrophys., 65, 89  
 Mathieu R. D., Latham D. W., 1986, AJ, 92, 1364  
 Nemec J. M., Cohen J. G., 1989, ApJ, 336, 780  
 Nemec J. M., Harris H. C., 1987, ApJ, 316, 172  
 Qian S.-B., Yang Y.-G., 2005, MNRAS, 356, 765  
 Qian S.-B., Yang Y.-G., Soonthornthum B., Zhu L.-Y., He J.-J., Yuan J.-Z., 2005, AJ, 130, 224  
 Rasio F. A., Shapiro S. L., 1995, ApJ, 438, 887  
 Richer H. B. et al., 2004, AJ, 127, 2771  
 Rubenstein E. P., 2001, AJ, 121, 3219  
 Rubenstein E. P., Bailyn C. D., 1996, AJ, 111, 260  
 Rucinski S. M., 1969, A&A, 19, 245  
 Rucinski S. M., 2000, AJ, 120, 319  
 Schmidt-Kaler Th., 1982, in Schaifers K., Voigt H. H., eds, Landolt-Bornstein: Numerical Data and Functional Relationships in Science and Technology, Vol. 2b. Springer-Verlag, Berlin  
 Wilson R. E., 1990, ApJ, 356, 613  
 Wilson R. E., 1994, PASP, 106, 921  
 Wilson R. E., Devinney E. J., 1971, ApJ, 166, 605  
 Wilson R. E., Van Hamme W., 2003, Computing Binary Stars Observables, 4th edn of the W-D program, available from ftp.astro.ufl.edu/pub/wilson/lcdc2003  
 Yakut K., Eggleton P. P., 2005, ApJ, 629, 1055  
 Yakut K., Kalomeni B., Ibanoglu C., 2004, A&A, 417, 725  
 Yang Y. G., Qian S. B., Zhu L. Y., 2005, AJ, 130, 2252  
 Yang Y.-L., Liu Q.-Y., 2003, New Astron., 8, 465  
 Yang Y.-G., Qian S.-B., Zhu L.-Y., He J.-J., 2009, AJ, 138, 540

## APPENDIX A: ORIGINAL DATA

**Table A1.** The original data of V47 in  $B$  band observed by 2.15-m telescope at CASLEO. Hel. JD 245 5300+.

Hel. JD	Phase	$\Delta m$	Errors	Hel. JD	Phase	$\Delta m$	Errors	Hel. JD	Phase	$\Delta m$	Errors
55.5069	0.4199	1.284	0.025	55.6040	0.7796	1.098	0.021	55.7012	0.1396	1.167	0.033
55.5083	0.4251	1.300	0.025	55.6054	0.7848	1.137	0.019	55.7026	0.1448	1.151	0.031
55.5097	0.4303	1.312	0.023	55.6069	0.7903	1.125	0.020	55.7041	0.1504	1.125	0.039
55.5112	0.4358	1.348	0.026	55.6083	0.7955	1.128	0.020	55.7055	0.1555	1.105	0.044
55.5126	0.4410	1.313	0.027	55.6098	0.8011	1.151	0.018	55.7070	0.1611	1.115	0.044
55.5140	0.4462	1.352	0.026	55.6112	0.8063	1.124	0.023	55.7084	0.1663	1.084	0.047
55.5155	0.4518	1.354	0.026	55.6126	0.8114	1.145	0.021	55.7099	0.1718	1.109	0.036
55.5169	0.4570	1.362	0.025	55.6141	0.8170	1.137	0.023	55.7113	0.1770	1.107	0.037
55.5183	0.4621	1.376	0.022	55.6155	0.8222	1.133	0.022	55.7127	0.1822	1.106	0.034
55.5198	0.4677	1.397	0.023	55.6170	0.8277	1.157	0.021	55.7142	0.1878	1.091	0.036
55.5219	0.4755	1.406	0.021	55.6184	0.8329	1.164	0.020	55.7156	0.1930	1.072	0.039
55.5233	0.4807	1.400	0.022	55.6198	0.8381	1.169	0.021	55.7171	0.1985	1.084	0.045
55.5248	0.4862	1.413	0.023	55.6213	0.8437	1.171	0.022	55.7185	0.2037	1.072	0.053
55.5262	0.4914	1.418	0.021	55.6227	0.8489	1.169	0.021	55.7199	0.2089	1.068	0.050
55.5276	0.4966	1.408	0.023	55.6241	0.8540	1.177	0.022	55.7214	0.2144	1.041	0.046
55.5291	0.5022	1.417	0.023	55.6256	0.8596	1.183	0.029	55.7228	0.2196	1.066	0.048
55.5305	0.5073	1.412	0.021	55.6270	0.8648	1.194	0.026	55.7252	0.2285	1.052	0.052
55.5319	0.5125	1.387	0.023	55.6284	0.8700	1.190	0.022	55.7281	0.2393	1.064	0.044
55.5334	0.5181	1.409	0.019	55.6299	0.8755	1.209	0.025	55.7295	0.2444	1.051	0.045
55.5348	0.5233	1.397	0.021	55.6313	0.8807	1.209	0.024	55.7310	0.2500	1.039	0.046
55.5362	0.5284	1.395	0.022	55.6327	0.8859	1.213	0.023	55.7324	0.2552	1.058	0.044
55.5377	0.5340	1.401	0.023	55.6342	0.8914	1.220	0.022	55.7338	0.2604	1.057	0.045
55.5391	0.5392	1.381	0.022	55.6356	0.8966	1.242	0.023	55.7353	0.2659	1.048	0.042
55.5406	0.5447	1.360	0.022	55.6370	0.9018	1.239	0.022	55.7367	0.2711	1.085	0.036
55.5420	0.5499	1.349	0.022	55.6385	0.9074	1.255	0.021	55.7382	0.2767	1.103	0.031
55.5435	0.5555	1.353	0.021	55.6399	0.9126	1.263	0.023	55.7396	0.2819	1.092	0.031
55.5449	0.5607	1.350	0.020	55.6414	0.9181	1.272	0.023	55.7410	0.2870	1.073	0.036
55.5464	0.5662	1.331	0.019	55.6428	0.9233	1.280	0.023	55.7425	0.2926	1.085	0.035
55.5478	0.5714	1.341	0.020	55.6443	0.9289	1.316	0.023	55.7439	0.2978	1.102	0.038
55.5493	0.5770	1.323	0.018	55.6457	0.9340	1.322	0.026	55.7454	0.3033	1.102	0.035
55.5507	0.5822	1.316	0.019	55.6472	0.9396	1.329	0.028	55.7468	0.3085	1.094	0.034
55.5522	0.5877	1.290	0.021	55.6486	0.9448	1.325	0.025	55.7483	0.3141	1.094	0.037
55.5536	0.5929	1.259	0.023	55.6501	0.9503	1.351	0.030	55.7497	0.3193	1.137	0.036
55.5551	0.5985	1.267	0.021	55.6526	0.9596	1.347	0.035	55.7512	0.3248	1.075	0.044
55.5565	0.6036	1.265	0.019	55.6539	0.9644	1.337	0.048	55.7526	0.3300	1.119	0.038
55.5579	0.6088	1.245	0.019	55.6553	0.9696	1.349	0.050	55.7541	0.3356	1.101	0.039
55.5594	0.6144	1.229	0.020	55.6566	0.9744	1.377	0.042	55.7555	0.3408	1.124	0.041
55.5608	0.6196	1.211	0.020	55.6579	0.9792	1.342	0.038	55.7570	0.3463	1.139	0.038
55.5622	0.6248	1.193	0.023	55.6593	0.9844	1.346	0.036	55.7584	0.3515	1.157	0.038
55.5637	0.6303	1.203	0.021	55.6606	0.9892	1.356	0.033	55.7599	0.3570	1.182	0.038
55.5651	0.6355	1.202	0.020	55.6619	0.9941	1.374	0.031	55.7613	0.3622	1.165	0.035
55.5665	0.6407	1.194	0.018	55.6632	0.9989	1.381	0.030	55.7627	0.3674	1.162	0.035
55.5680	0.6462	1.171	0.018	55.6645	0.0037	1.384	0.030	55.7642	0.3730	1.188	0.035
55.5694	0.6514	1.162	0.020	55.6667	0.0118	1.346	0.032	55.7656	0.3782	1.179	0.041
55.5709	0.6570	1.170	0.019	55.6681	0.0170	1.360	0.028	55.7670	0.3833	1.160	0.046
55.5723	0.6622	1.152	0.021	55.6695	0.0222	1.361	0.028	55.7685	0.3889	1.199	0.045
55.5737	0.6674	1.157	0.021	55.6710	0.0278	1.360	0.027	55.7699	0.3941	1.225	0.040
55.5752	0.6729	1.148	0.021	55.6724	0.0329	1.352	0.027	55.7713	0.3993	1.229	0.038
55.5766	0.6781	1.152	0.020	55.6738	0.0381	1.341	0.028	55.7728	0.4048	1.231	0.041
55.5780	0.6833	1.147	0.022	55.6753	0.0437	1.343	0.030	55.7742	0.4100	1.252	0.043
55.5795	0.6888	1.130	0.022	55.6767	0.0489	1.330	0.031	55.7757	0.4156	1.274	0.040
55.5809	0.6940	1.138	0.021	55.6781	0.0541	1.298	0.035	55.7771	0.4208	1.268	0.035
55.5823	0.6992	1.133	0.021	55.6796	0.0596	1.313	0.033	55.7785	0.4259	1.286	0.039
55.5838	0.7048	1.104	0.023	55.6810	0.0648	1.316	0.034	55.7800	0.4315	1.294	0.051
55.5852	0.7099	1.125	0.021	55.6824	0.0700	1.309	0.040	55.7814	0.4367	1.289	0.044
55.5866	0.7151	1.107	0.022	55.6839	0.0755	1.281	0.035	55.7828	0.4419	1.343	0.051
55.5881	0.7207	1.102	0.024	55.6853	0.0807	1.263	0.033	55.7843	0.4474	1.333	0.053
55.5895	0.7259	1.116	0.025	55.6868	0.0863	1.208	0.034	55.7857	0.4526	1.334	0.045
55.5910	0.7314	1.102	0.024	55.6882	0.0915	1.218	0.045	55.7871	0.4578	1.338	0.048
55.5924	0.7366	1.110	0.024	55.6896	0.0967	1.174	0.044	55.7886	0.4634	1.331	0.048
55.5939	0.7422	1.109	0.027	55.6911	0.1022	1.206	0.038	55.7900	0.4685	1.308	0.050
55.5953	0.7474	1.121	0.025	55.6925	0.1074	1.178	0.037	55.7915	0.4741	1.330	0.053
55.5968	0.7529	1.108	0.024	55.6940	0.1130	1.192	0.035	55.7929	0.4793	1.340	0.053
55.5982	0.7581	1.107	0.026	55.6954	0.1181	1.192	0.031	55.7943	0.4845	1.366	0.057
55.5996	0.7633	1.114	0.025	55.6969	0.1237	1.186	0.033	55.7958	0.4900	1.355	0.050
55.6011	0.7688	1.090	0.022	55.6983	0.1289	1.165	0.033				
55.6025	0.7740	1.093	0.023	55.6998	0.1344	1.150	0.034				

**Table A2.** The original data of V47 in *V* band observed by 2.15-m telescope at CASLEO. Hel. JD 245 5300+

Hel. JD	Phase	$\Delta m$	Errors	Hel. JD	Phase	$\Delta m$	Errors	Hel. JD	Phase	$\Delta m$	Errors
54.5267	0.7892	1.424	0.023	54.6287	0.1670	1.454	0.018	54.7253	0.5248	1.671	0.028
54.5278	0.7933	1.429	0.025	54.6298	0.1711	1.452	0.018	54.7264	0.5289	1.677	0.028
54.5289	0.7973	1.431	0.023	54.6309	0.1752	1.442	0.020	54.7275	0.5330	1.679	0.031
54.5299	0.8010	1.426	0.019	54.6319	0.1789	1.433	0.019	54.7286	0.5370	1.679	0.029
54.5310	0.8051	1.435	0.019	54.6330	0.1829	1.435	0.020	54.7296	0.5407	1.654	0.029
54.5320	0.8088	1.428	0.019	54.6340	0.1866	1.428	0.022	54.7307	0.5448	1.650	0.028
54.5331	0.8129	1.435	0.019	54.6351	0.1907	1.422	0.022	54.7318	0.5489	1.669	0.030
54.5342	0.8170	1.433	0.019	54.6362	0.1948	1.418	0.023	54.7328	0.5526	1.628	0.028
54.5352	0.8207	1.447	0.019	54.6372	0.1985	1.421	0.020	54.7339	0.5567	1.618	0.034
54.5363	0.8247	1.451	0.019	54.6383	0.2026	1.422	0.021	54.7350	0.5607	1.632	0.030
54.5476	0.8666	1.484	0.019	54.6394	0.2066	1.415	0.021	54.7360	0.5645	1.617	0.032
54.5487	0.8707	1.501	0.020	54.6404	0.2103	1.407	0.021	54.7371	0.5685	1.599	0.033
54.5498	0.8748	1.512	0.018	54.6415	0.2144	1.413	0.018	54.7382	0.5726	1.606	0.028
54.5508	0.8785	1.509	0.019	54.6426	0.2185	1.407	0.021	54.7393	0.5767	1.584	0.030
54.5519	0.8825	1.507	0.021	54.6453	0.2285	1.407	0.021	54.7403	0.5804	1.573	0.032
54.5530	0.8866	1.509	0.020	54.6464	0.2326	1.411	0.019	54.7414	0.5845	1.573	0.035
54.5540	0.8903	1.526	0.020	54.6474	0.2363	1.394	0.021	54.7425	0.5885	1.566	0.036
54.5551	0.8944	1.529	0.020	54.6485	0.2403	1.407	0.021	54.7435	0.5922	1.581	0.035
54.5562	0.8985	1.523	0.020	54.6496	0.2444	1.401	0.021	54.7446	0.5963	1.540	0.040
54.5573	0.9025	1.550	0.021	54.6506	0.2481	1.408	0.021	54.7457	0.6004	1.553	0.036
54.5583	0.9062	1.562	0.019	54.6517	0.2522	1.409	0.018	54.7468	0.6045	1.511	0.035
54.5594	0.9103	1.561	0.020	54.6528	0.2563	1.406	0.021	54.7478	0.6082	1.525	0.032
54.5604	0.9140	1.561	0.021	54.6538	0.2600	1.401	0.021	54.7489	0.6122	1.517	0.039
54.5615	0.9181	1.573	0.023	54.6549	0.2641	1.406	0.021	54.7500	0.6163	1.498	0.035
54.5626	0.9222	1.573	0.025	54.6560	0.2681	1.393	0.021	54.7510	0.6200	1.493	0.038
54.5636	0.9259	1.590	0.024	54.6570	0.2718	1.401	0.022	54.7529	0.6271	1.512	0.031
54.5647	0.9299	1.592	0.024	54.6581	0.2759	1.416	0.022	54.7539	0.6308	1.473	0.039
54.5658	0.9340	1.608	0.024	54.6592	0.2800	1.412	0.023	54.7550	0.6348	1.483	0.039
54.5668	0.9377	1.613	0.026	54.6602	0.2837	1.410	0.022	54.7561	0.6389	1.479	0.036
54.5679	0.9418	1.625	0.022	54.6613	0.2878	1.397	0.026	54.7571	0.6426	1.452	0.037
54.5690	0.9459	1.619	0.022	54.6624	0.2918	1.407	0.027	54.7582	0.6467	1.454	0.038
54.5700	0.9496	1.639	0.022	54.6634	0.2955	1.413	0.023	54.7593	0.6508	1.473	0.038
54.5711	0.9537	1.641	0.023	54.6645	0.2996	1.414	0.023	54.7603	0.6545	1.457	0.036
54.5722	0.9577	1.650	0.022	54.6656	0.3037	1.413	0.024	54.7625	0.6626	1.434	0.043
54.5732	0.9614	1.671	0.022	54.6666	0.3074	1.417	0.024	54.7635	0.6663	1.451	0.043
54.5743	0.9655	1.659	0.020	54.6677	0.3115	1.434	0.023	54.7646	0.6704	1.449	0.043
54.5754	0.9696	1.667	0.023	54.6688	0.3155	1.418	0.022	54.7657	0.6745	1.412	0.045
54.5764	0.9733	1.654	0.020	54.6699	0.3196	1.425	0.022	54.7667	0.6782	1.418	0.045
54.5775	0.9774	1.673	0.023	54.6709	0.3233	1.428	0.023	54.7678	0.6822	1.432	0.051
54.5785	0.9811	1.668	0.023	54.6720	0.3274	1.438	0.025	54.7688	0.6859	1.432	0.048
54.5796	0.9851	1.666	0.024	54.6731	0.3315	1.432	0.026	54.7699	0.6900	1.400	0.043
54.5807	0.9892	1.667	0.021	54.6741	0.3352	1.450	0.027	54.7710	0.6941	1.415	0.040
54.5817	0.9929	1.667	0.028	54.6752	0.3392	1.449	0.025	54.7720	0.6978	1.398	0.043
54.5828	0.9970	1.662	0.024	54.6763	0.3433	1.453	0.026	54.7731	0.7019	1.421	0.049
54.5839	0.0011	1.666	0.023	54.6774	0.3474	1.457	0.026	54.7742	0.7059	1.405	0.048
54.5849	0.0048	1.669	0.021	54.6784	0.3511	1.473	0.025	54.7752	0.7097	1.426	0.046
54.5860	0.0088	1.671	0.021	54.6795	0.3552	1.472	0.025	54.7763	0.7137	1.409	0.048
54.5871	0.0129	1.674	0.022	54.6806	0.3592	1.484	0.026	54.7774	0.7178	1.395	0.046
54.5881	0.0166	1.664	0.024	54.6816	0.3630	1.480	0.025	54.7784	0.7215	1.399	0.048
54.5892	0.0207	1.667	0.022	54.6827	0.3670	1.500	0.025	54.7795	0.7256	1.398	0.046
54.5903	0.0248	1.670	0.023	54.6838	0.3711	1.486	0.025	54.7806	0.7297	1.431	0.053
54.5913	0.0285	1.667	0.022	54.6849	0.3752	1.482	0.025	54.7816	0.7334	1.434	0.050
54.5924	0.0325	1.664	0.023	54.6859	0.3789	1.492	0.026	54.7838	0.7415	1.405	0.045
54.5935	0.0366	1.650	0.021	54.6870	0.3830	1.513	0.025	54.7848	0.7452	1.420	0.050
54.5945	0.0403	1.640	0.021	54.6881	0.3870	1.519	0.025	54.7859	0.7493	1.391	0.046
54.5956	0.0444	1.638	0.020	54.6891	0.3907	1.519	0.028	54.7870	0.7534	1.424	0.050
54.5967	0.0485	1.640	0.021	54.6902	0.3948	1.522	0.028	54.7880	0.7571	1.384	0.046
54.5977	0.0522	1.640	0.019	54.6912	0.3985	1.552	0.029	54.7891	0.7611	1.406	0.052
54.5988	0.0563	1.627	0.019	54.6923	0.4026	1.546	0.029	54.7902	0.7652	1.407	0.052
54.5999	0.0603	1.600	0.021	54.6934	0.4067	1.568	0.031	54.7923	0.7730	1.428	0.055
54.6009	0.0640	1.609	0.025	54.6944	0.4104	1.547	0.028	54.7934	0.7771	1.416	0.059
54.6020	0.0681	1.601	0.021	54.6955	0.4144	1.574	0.031	54.7944	0.7808	1.438	0.057
54.6031	0.0722	1.584	0.021	54.6966	0.4185	1.578	0.034	54.7955	0.7848	1.457	0.054

**Table A2 – continued**

Hel. JD	Phase	$\Delta m$	Errors	Hel. JD	Phase	$\Delta m$	Errors	Hel. JD	Phase	$\Delta m$	Errors
54.6041	0.0759	1.571	0.020	54.6976	0.4222	1.581	0.032	54.7966	0.7889	1.409	0.051
54.6052	0.0800	1.564	0.021	54.6987	0.4263	1.588	0.029	54.7987	0.7967	1.447	0.060
54.6063	0.0840	1.559	0.020	54.6998	0.4304	1.603	0.030	54.7998	0.8008	1.458	0.052
54.6074	0.0881	1.546	0.018	54.7008	0.4341	1.607	0.028	54.8009	0.8048	1.426	0.048
54.6084	0.0918	1.551	0.021	54.7019	0.4381	1.602	0.031	54.8019	0.8086	1.449	0.052
54.6095	0.0959	1.546	0.021	54.7030	0.4422	1.615	0.029	54.8030	0.8126	1.442	0.052
54.6106	0.1000	1.535	0.020	54.7040	0.4459	1.629	0.028	54.8041	0.8167	1.455	0.052
54.6116	0.1037	1.536	0.020	54.7051	0.4500	1.631	0.028	54.8052	0.8208	1.432	0.048
54.6127	0.1077	1.522	0.021	54.7062	0.4541	1.647	0.027	54.8062	0.8245	1.452	0.049
54.6138	0.1118	1.520	0.019	54.7072	0.4578	1.652	0.026	54.8073	0.8286	1.443	0.048
54.6148	0.1155	1.507	0.021	54.7083	0.4618	1.667	0.028	54.8105	0.8404	1.445	0.050
54.6159	0.1196	1.505	0.022	54.7093	0.4656	1.654	0.028	54.8127	0.8486	1.477	0.047
54.6170	0.1237	1.482	0.021	54.7104	0.4696	1.664	0.033	54.8137	0.8523	1.449	0.050
54.6181	0.1277	1.482	0.021	54.7115	0.4737	1.672	0.032	54.8158	0.8600	1.466	0.048
54.6191	0.1314	1.488	0.023	54.7147	0.4856	1.689	0.033	54.8169	0.8641	1.515	0.052
54.6202	0.1355	1.482	0.021	54.7157	0.4893	1.664	0.033	54.8180	0.8682	1.472	0.052
54.6213	0.1396	1.481	0.018	54.7168	0.4933	1.682	0.030	54.8190	0.8719	1.497	0.052
54.6223	0.1433	1.479	0.019	54.7179	0.4974	1.687	0.028	54.8201	0.8760	1.508	0.051
54.6234	0.1474	1.467	0.018	54.7189	0.5011	1.678	0.034	54.8212	0.8800	1.528	0.054
54.6245	0.1514	1.466	0.021	54.7211	0.5093	1.691	0.027	54.8222	0.8837	1.508	0.054
54.6255	0.1552	1.466	0.019	54.7221	0.5130	1.670	0.028	54.8233	0.8878	1.532	0.057
54.6266	0.1592	1.444	0.019	54.7232	0.5170	1.652	0.032	54.8244	0.8919	1.548	0.051
54.6277	0.1633	1.454	0.019	54.7243	0.5211	1.673	0.030	54.8318	0.9193	1.586	0.059

**Table A3.** The original data of V47 in R band observed by 2.15-m telescope at CASLEO. Hel. JD 245 5300+.

Hel. JD	Phase	$\Delta m$	Errors	Hel. JD	Phase	$\Delta m$	Errors	Hel. JD	Phase	$\Delta m$	Errors
52.6230	0.7378	1.572	0.016	52.7513	0.2130	1.552	0.021	52.8298	0.5038	1.796	0.025
52.6241	0.7418	1.559	0.016	52.7524	0.2171	1.548	0.021	52.8309	0.5078	1.829	0.024
52.6252	0.7459	1.551	0.016	52.7535	0.2211	1.538	0.021	52.8320	0.5119	1.822	0.021
52.6263	0.7500	1.553	0.016	52.7546	0.2252	1.559	0.021	52.8331	0.5160	1.816	0.023
52.6328	0.7741	1.564	0.016	52.7557	0.2293	1.534	0.022	52.8342	0.5201	1.810	0.023
52.6339	0.7781	1.551	0.016	52.7567	0.2330	1.535	0.023	52.8353	0.5241	1.818	0.024
52.6350	0.7822	1.556	0.017	52.7578	0.2371	1.544	0.025	52.8364	0.5282	1.811	0.025
52.6361	0.7863	1.561	0.016	52.7589	0.2411	1.530	0.028	52.8375	0.5323	1.809	0.027
52.6372	0.7903	1.560	0.017	52.7600	0.2452	1.532	0.021	52.8386	0.5363	1.807	0.026
52.6383	0.7944	1.553	0.018	52.7611	0.2493	1.528	0.022	52.8397	0.5404	1.823	0.028
52.6553	0.8574	1.619	0.020	52.7622	0.2534	1.530	0.021	52.8408	0.5445	1.781	0.025
52.6564	0.8615	1.613	0.020	52.7633	0.2574	1.533	0.021	52.8419	0.5486	1.785	0.028
52.6575	0.8655	1.621	0.018	52.7644	0.2615	1.524	0.023	53.6632	0.5907	1.675	0.018
52.6586	0.8696	1.642	0.018	52.7655	0.2656	1.534	0.021	53.6643	0.5948	1.664	0.021
52.6597	0.8737	1.629	0.017	52.7666	0.2697	1.540	0.025	53.6653	0.5985	1.667	0.018
52.6706	0.9141	1.707	0.017	52.7677	0.2737	1.536	0.021	53.6664	0.6026	1.661	0.020
52.6717	0.9181	1.721	0.018	52.7688	0.2778	1.543	0.021	53.6675	0.6067	1.659	0.021
52.6727	0.9218	1.736	0.018	52.7699	0.2819	1.534	0.023	53.6686	0.6107	1.640	0.019
52.6738	0.9259	1.737	0.019	52.7710	0.2860	1.528	0.026	53.6732	0.6278	1.608	0.022
52.6749	0.9300	1.735	0.017	52.7721	0.2900	1.542	0.034	53.6743	0.6318	1.616	0.024
52.6825	0.9581	1.791	0.018	52.7732	0.2941	1.534	0.031	53.6754	0.6359	1.611	0.020
52.6836	0.9622	1.788	0.018	52.7743	0.2982	1.534	0.029	53.6801	0.6533	1.577	0.026
52.6847	0.9663	1.796	0.018	52.7754	0.3023	1.548	0.028	53.6811	0.6570	1.575	0.025
52.6857	0.9700	1.802	0.019	52.7765	0.3063	1.539	0.024	53.6822	0.6611	1.574	0.019
52.6868	0.9741	1.809	0.021	52.7776	0.3104	1.546	0.033	53.6868	0.6781	1.548	0.023
52.6941	0.0011	1.812	0.020	52.7787	0.3145	1.561	0.030	53.6879	0.6822	1.548	0.021
52.6952	0.0052	1.805	0.019	52.7798	0.3186	1.560	0.031	53.6890	0.6863	1.550	0.021
52.6963	0.0093	1.807	0.021	52.7809	0.3226	1.563	0.032	53.6937	0.7037	1.521	0.037
52.6974	0.0133	1.813	0.021	52.7820	0.3267	1.573	0.028	53.6947	0.7074	1.521	0.028
52.6985	0.0174	1.811	0.021	52.7831	0.3308	1.568	0.028	53.6958	0.7115	1.528	0.025
52.7061	0.0456	1.794	0.020	52.7842	0.3348	1.585	0.028	53.7019	0.7341	1.522	0.025
52.7072	0.0496	1.768	0.020	52.7874	0.3467	1.589	0.025	53.7029	0.7378	1.536	0.021

**Table A3 – continued**

Hel. JD	Phase	$\Delta m$	Errors	Hel. JD	Phase	$\Delta m$	Errors	Hel. JD	Phase	$\Delta m$	Errors
52.7083	0.0537	1.766	0.021	52.7885	0.3508	1.604	0.026	53.7040	0.7419	1.530	0.024
52.7094	0.0578	1.763	0.022	52.7896	0.3548	1.603	0.023	53.7087	0.7593	1.528	0.025
52.7105	0.0619	1.756	0.020	52.7907	0.3589	1.612	0.024	53.7097	0.7630	1.527	0.024
52.7122	0.0682	1.744	0.020	52.7918	0.3630	1.619	0.025	53.7108	0.7670	1.539	0.022
52.7133	0.0722	1.735	0.021	52.7928	0.3667	1.613	0.027	53.7199	0.8007	1.545	0.021
52.7144	0.0763	1.730	0.020	52.7939	0.3708	1.646	0.031	53.7210	0.8048	1.554	0.019
52.7155	0.0804	1.715	0.021	52.7950	0.3749	1.621	0.028	53.7221	0.8089	1.548	0.018
52.7166	0.0845	1.701	0.022	52.7961	0.3789	1.636	0.026	53.7233	0.8133	1.551	0.018
52.7192	0.0941	1.682	0.018	52.7972	0.3830	1.636	0.025	53.7243	0.8170	1.568	0.019
52.7203	0.0982	1.673	0.021	52.7993	0.3908	1.667	0.025	53.7254	0.8211	1.558	0.017
52.7214	0.1022	1.668	0.020	52.8004	0.3949	1.668	0.024	53.7266	0.8256	1.569	0.017
52.7225	0.1063	1.656	0.021	52.8015	0.3989	1.671	0.028	53.7276	0.8293	1.575	0.018
52.7236	0.1104	1.657	0.018	52.8025	0.4026	1.688	0.023	53.7287	0.8333	1.574	0.019
52.7247	0.1145	1.649	0.018	52.8036	0.4067	1.680	0.027	53.7384	0.8693	1.618	0.018
52.7258	0.1185	1.648	0.018	52.8047	0.4108	1.693	0.024	53.7395	0.8733	1.614	0.019
52.7269	0.1226	1.642	0.017	52.8058	0.4149	1.693	0.037	53.7406	0.8774	1.629	0.020
52.7280	0.1267	1.640	0.017	52.8069	0.4189	1.700	0.032	53.7419	0.8822	1.626	0.023
52.7290	0.1304	1.623	0.016	52.8080	0.4230	1.710	0.028	53.7430	0.8863	1.629	0.025
52.7301	0.1345	1.622	0.019	52.8091	0.4271	1.713	0.037	53.7501	0.9126	1.665	0.034
52.7312	0.1385	1.610	0.018	52.8102	0.4312	1.730	0.030	53.7511	0.9163	1.684	0.027
52.7323	0.1426	1.621	0.018	52.8112	0.4349	1.742	0.028	53.7522	0.9204	1.686	0.023
52.7334	0.1467	1.596	0.019	52.8123	0.4389	1.748	0.033	53.7533	0.9245	1.686	0.027
52.7345	0.1508	1.598	0.019	52.8134	0.4430	1.780	0.031	53.7543	0.9282	1.705	0.027
52.7356	0.1548	1.603	0.020	52.8145	0.4471	1.765	0.029	53.7654	0.9693	1.781	0.033
52.7367	0.1589	1.587	0.020	52.8156	0.4512	1.779	0.026	53.7665	0.9734	1.784	0.036
52.7377	0.1626	1.587	0.020	52.8167	0.4552	1.799	0.026	53.7746	0.0034	1.788	0.024
52.7388	0.1667	1.578	0.019	52.8178	0.4593	1.807	0.031	53.7756	0.0071	1.792	0.026
52.7399	0.1708	1.576	0.019	52.8189	0.4634	1.811	0.026	53.7767	0.0111	1.797	0.025
52.7415	0.1767	1.577	0.019	52.8199	0.4671	1.822	0.025	53.7777	0.0148	1.792	0.033
52.7426	0.1808	1.580	0.019	52.8210	0.4712	1.819	0.025	53.7788	0.0189	1.790	0.027
52.7437	0.1848	1.580	0.019	52.8221	0.4752	1.800	0.028	53.7874	0.0508	1.746	0.027
52.7448	0.1889	1.577	0.019	52.8232	0.4793	1.812	0.030	53.7884	0.0545	1.742	0.026
52.7459	0.1930	1.554	0.022	52.8243	0.4834	1.809	0.026	53.7895	0.0585	1.747	0.026
52.7469	0.1967	1.556	0.020	52.8254	0.4875	1.835	0.023	53.7955	0.0808	1.688	0.033
52.7480	0.2008	1.545	0.022	52.8265	0.4915	1.810	0.024	53.7965	0.0845	1.692	0.034
52.7491	0.2048	1.550	0.019	52.8276	0.4956	1.808	0.025				
52.7502	0.2089	1.533	0.023	52.8287	0.4997	1.817	0.024				

**Table A4.** The original data of V47 in  $I$  band observed by 2.15-m telescope at CASLEO. Hel. JD 245 5300+.

Hel. JD	Phase	$\Delta m$	Errors	Hel. JD	Phase	$\Delta m$	Errors	Hel. JD	Phase	$\Delta m$	Errors
52.6402	0.8015	1.678	0.018	53.5693	0.2429	1.631	0.021	53.6491	0.5385	1.889	0.024
52.6413	0.8055	1.696	0.020	53.5704	0.2470	1.648	0.020	53.6502	0.5426	1.886	0.022
52.6424	0.8096	1.693	0.019	53.5714	0.2507	1.641	0.022	53.6512	0.5463	1.882	0.021
52.6435	0.8137	1.683	0.018	53.5725	0.2548	1.634	0.021	53.6523	0.5504	1.879	0.022
52.6446	0.8178	1.684	0.019	53.5736	0.2588	1.629	0.021	53.6534	0.5544	1.866	0.021
52.6457	0.8218	1.690	0.018	53.5746	0.2625	1.640	0.020	53.6544	0.5581	1.864	0.022
52.6468	0.8259	1.701	0.020	53.5757	0.2666	1.650	0.019	53.6559	0.5637	1.850	0.020
52.6479	0.8300	1.701	0.020	53.5768	0.2707	1.645	0.019	53.6569	0.5674	1.828	0.020
52.6490	0.8341	1.700	0.018	53.5778	0.2744	1.637	0.019	53.6580	0.5715	1.831	0.022
52.6501	0.8381	1.713	0.019	53.5789	0.2785	1.651	0.019	53.6591	0.5755	1.828	0.022
52.6626	0.8844	1.760	0.020	53.5799	0.2822	1.647	0.018	53.6601	0.5792	1.822	0.019
52.6637	0.8885	1.767	0.019	53.5810	0.2863	1.664	0.017	53.6612	0.5833	1.810	0.019
52.6648	0.8926	1.769	0.020	53.5821	0.2903	1.655	0.018	53.6699	0.6155	1.758	0.019
52.6659	0.8967	1.772	0.019	53.5831	0.2940	1.648	0.018	53.6709	0.6192	1.748	0.019
52.6670	0.9007	1.788	0.019	53.5842	0.2981	1.656	0.019	53.6720	0.6233	1.737	0.020

**Table A4** – *continued*

Hel. JD	Phase	$\Delta m$	Errors	Hel. JD	Phase	$\Delta m$	Errors	Hel. JD	Phase	$\Delta m$	Errors
52.6767	0.9367	1.867	0.021	53.5853	0.3022	1.660	0.019	53.6767	0.6407	1.722	0.022
52.6777	0.9404	1.887	0.021	53.5863	0.3059	1.671	0.019	53.6778	0.6448	1.723	0.021
52.6788	0.9444	1.883	0.021	53.5874	0.3100	1.660	0.020	53.6788	0.6485	1.716	0.021
52.6799	0.9485	1.889	0.021	53.5885	0.3140	1.660	0.020	53.6834	0.6655	1.692	0.021
52.6810	0.9526	1.899	0.021	53.5895	0.3177	1.668	0.021	53.6845	0.6696	1.681	0.022
52.6882	0.9793	1.916	0.021	53.5906	0.3218	1.684	0.019	53.6856	0.6737	1.675	0.022
52.6892	0.9830	1.922	0.021	53.5917	0.3259	1.678	0.019	53.6903	0.6911	1.670	0.021
52.6903	0.9870	1.923	0.020	53.5927	0.3296	1.674	0.020	53.6914	0.6952	1.669	0.020
52.6914	0.9911	1.931	0.021	53.5938	0.3337	1.683	0.021	53.6924	0.6989	1.671	0.019
52.6925	0.9952	1.912	0.020	53.5949	0.3377	1.677	0.018	53.6971	0.7163	1.644	0.026
52.7000	0.0230	1.933	0.022	53.5959	0.3414	1.695	0.019	53.6982	0.7204	1.654	0.024
52.7011	0.0270	1.914	0.022	53.5970	0.3455	1.680	0.019	53.6993	0.7244	1.631	0.028
52.7022	0.0311	1.912	0.022	53.5981	0.3496	1.698	0.019	53.7053	0.7467	1.654	0.026
52.7033	0.0352	1.919	0.022	53.6013	0.3614	1.707	0.019	53.7063	0.7504	1.658	0.026
52.7044	0.0393	1.905	0.021	53.6024	0.3655	1.733	0.021	53.7074	0.7544	1.657	0.025
53.5239	0.0747	1.825	0.024	53.6035	0.3696	1.732	0.019	53.7121	0.7719	1.661	0.019
53.5249	0.0785	1.806	0.023	53.6046	0.3737	1.721	0.019	53.7132	0.7759	1.657	0.019
53.5260	0.0825	1.795	0.024	53.6056	0.3774	1.738	0.020	53.7143	0.7800	1.661	0.019
53.5270	0.0862	1.799	0.026	53.6067	0.3814	1.738	0.020	53.7164	0.7878	1.661	0.019
53.5281	0.0903	1.800	0.030	53.6078	0.3855	1.746	0.021	53.7174	0.7915	1.664	0.019
53.5292	0.0944	1.781	0.026	53.6089	0.3896	1.748	0.019	53.7185	0.7956	1.677	0.021
53.5302	0.0981	1.769	0.026	53.6099	0.3933	1.758	0.021	53.7315	0.8437	1.710	0.020
53.5313	0.1022	1.742	0.024	53.6110	0.3974	1.770	0.021	53.7325	0.8474	1.716	0.019
53.5324	0.1062	1.747	0.023	53.6128	0.4040	1.779	0.021	53.7336	0.8515	1.719	0.019
53.5334	0.1099	1.738	0.026	53.6139	0.4081	1.789	0.021	53.7347	0.8556	1.715	0.019
53.5345	0.1140	1.738	0.021	53.6149	0.4118	1.790	0.023	53.7358	0.8596	1.733	0.019
53.5356	0.1181	1.727	0.023	53.6160	0.4159	1.802	0.022	53.7369	0.8637	1.727	0.020
53.5367	0.1222	1.716	0.023	53.6171	0.4200	1.811	0.022	53.7445	0.8919	1.773	0.022
53.5377	0.1259	1.709	0.025	53.6182	0.4240	1.812	0.022	53.7456	0.8959	1.765	0.023
53.5388	0.1299	1.710	0.023	53.6192	0.4277	1.832	0.022	53.7467	0.9000	1.790	0.022
53.5399	0.1340	1.712	0.025	53.6203	0.4318	1.837	0.022	53.7477	0.9037	1.792	0.025
53.5410	0.1381	1.718	0.022	53.6214	0.4359	1.842	0.022	53.7488	0.9078	1.786	0.030
53.5420	0.1418	1.690	0.021	53.6224	0.4396	1.853	0.021	53.7595	0.9474	1.860	0.028
53.5431	0.1459	1.695	0.022	53.6235	0.4437	1.869	0.022	53.7606	0.9515	1.865	0.029
53.5442	0.1499	1.687	0.023	53.6246	0.4477	1.861	0.025	53.7616	0.9552	1.877	0.030
53.5454	0.1544	1.679	0.025	53.6257	0.4518	1.875	0.022	53.7627	0.9593	1.893	0.025
53.5465	0.1585	1.674	0.024	53.6267	0.4555	1.881	0.024	53.7638	0.9634	1.906	0.026
53.5476	0.1625	1.694	0.022	53.6278	0.4596	1.889	0.022	53.7699	0.9859	1.932	0.035
53.5486	0.1662	1.681	0.023	53.6289	0.4637	1.896	0.022	53.7710	0.9900	1.908	0.028
53.5497	0.1703	1.682	0.021	53.6299	0.4674	1.916	0.023	53.7721	0.9941	1.911	0.034
53.5508	0.1744	1.678	0.021	53.6310	0.4715	1.901	0.022	53.7731	0.9978	1.922	0.031
53.5518	0.1781	1.681	0.021	53.6321	0.4755	1.903	0.023	53.7817	0.0297	1.915	0.031
53.5529	0.1822	1.672	0.019	53.6331	0.4792	1.910	0.021	53.7827	0.0334	1.898	0.028
53.5540	0.1862	1.660	0.019	53.6342	0.4833	1.921	0.022	53.7838	0.0374	1.904	0.031
53.5551	0.1903	1.676	0.022	53.6352	0.4870	1.916	0.022	53.7849	0.0415	1.913	0.031
53.5562	0.1944	1.670	0.019	53.6363	0.4911	1.904	0.022	53.7859	0.0452	1.896	0.027
53.5572	0.1981	1.658	0.019	53.6374	0.4952	1.919	0.022	53.7919	0.0674	1.842	0.039
53.5583	0.2022	1.649	0.021	53.6384	0.4989	1.916	0.023	53.7929	0.0711	1.841	0.035
53.5594	0.2062	1.646	0.022	53.6395	0.5029	1.900	0.025	53.7940	0.0752	1.832	0.029
53.5604	0.2099	1.627	0.020	53.6406	0.5070	1.914	0.023	53.7995	0.0956	1.798	0.031
53.5615	0.2140	1.653	0.020	53.6416	0.5107	1.896	0.022	53.8006	0.0997	1.802	0.038
53.5626	0.2181	1.639	0.021	53.6427	0.5148	1.909	0.023	53.8094	0.1323	1.742	0.030
53.5636	0.2218	1.647	0.019	53.6438	0.5189	1.905	0.023	53.8137	0.1482	1.707	0.035
53.5647	0.2259	1.639	0.021	53.6448	0.5226	1.910	0.022	53.8234	0.1841	1.660	0.036
53.5658	0.2299	1.637	0.018	53.6459	0.5266	1.915	0.023	53.8255	0.1919	1.648	0.037
53.5672	0.2351	1.635	0.018	53.6470	0.5307	1.900	0.024				
53.5682	0.2388	1.639	0.020	53.6480	0.5344	1.876	0.025				

**Table A5.** The original data of V53 in  $B$  band observed by 2.15-m telescope at CASLEO. Hel. JD 245 5300+.

Hel. JD	Phase	$\Delta m$	Errors	Hel. JD	Phase	$\Delta m$	Errors	Hel. JD	Phase	$\Delta m$	Errors
55.5069	0.0776	-1.184	0.036	55.6025	0.3875	-1.312	0.034	55.6998	0.7029	-1.311	0.041
55.5083	0.0822	-1.186	0.037	55.6040	0.3924	-1.294	0.034	55.7012	0.7074	-1.307	0.040
55.5097	0.0867	-1.188	0.037	55.6054	0.3969	-1.315	0.034	55.7026	0.7120	-1.312	0.039
55.5112	0.0916	-1.177	0.038	55.6069	0.4018	-1.291	0.034	55.7041	0.7168	-1.322	0.042
55.5126	0.0961	-1.178	0.038	55.6083	0.4063	-1.285	0.034	55.7055	0.7214	-1.320	0.049
55.5140	0.1006	-1.178	0.038	55.6098	0.4112	-1.298	0.034	55.7070	0.7262	-1.314	0.051
55.5155	0.1055	-1.189	0.036	55.6112	0.4157	-1.266	0.036	55.7084	0.7308	-1.321	0.054
55.5169	0.1100	-1.170	0.037	55.6126	0.4202	-1.286	0.034	55.7099	0.7356	-1.344	0.044
55.5183	0.1146	-1.208	0.037	55.6141	0.4251	-1.276	0.034	55.7113	0.7402	-1.319	0.043
55.5198	0.1194	-1.205	0.037	55.6155	0.4296	-1.270	0.034	55.7127	0.7447	-1.343	0.043
55.5219	0.1262	-1.218	0.035	55.6170	0.4345	-1.269	0.034	55.7142	0.7496	-1.331	0.043
55.5233	0.1308	-1.240	0.035	55.6184	0.4390	-1.259	0.035	55.7156	0.7541	-1.329	0.044
55.5248	0.1356	-1.236	0.035	55.6198	0.4436	-1.252	0.035	55.7171	0.7590	-1.336	0.052
55.5262	0.1402	-1.230	0.035	55.6213	0.4484	-1.251	0.035	55.7185	0.7635	-1.324	0.065
55.5276	0.1447	-1.240	0.035	55.6227	0.4530	-1.242	0.035	55.7199	0.7680	-1.314	0.065
55.5291	0.1496	-1.253	0.034	55.6241	0.4575	-1.244	0.035	55.7214	0.7729	-1.333	0.056
55.5305	0.1541	-1.262	0.034	55.6256	0.4624	-1.226	0.041	55.7228	0.7774	-1.337	0.057
55.5319	0.1587	-1.272	0.034	55.6270	0.4669	-1.250	0.037	55.7252	0.7852	-1.315	0.061
55.5334	0.1635	-1.282	0.034	55.6284	0.4715	-1.221	0.036	55.7267	0.7901	-1.342	0.065
55.5348	0.1681	-1.278	0.034	55.6299	0.4763	-1.211	0.037	55.7281	0.7946	-1.341	0.051
55.5362	0.1726	-1.271	0.034	55.6313	0.4809	-1.195	0.037	55.7295	0.7992	-1.328	0.053
55.5377	0.1775	-1.293	0.034	55.6327	0.4854	-1.205	0.036	55.7310	0.8040	-1.349	0.050
55.5391	0.1820	-1.289	0.033	55.6342	0.4903	-1.200	0.035	55.7324	0.8086	-1.355	0.051
55.5406	0.1869	-1.287	0.034	55.6356	0.4948	-1.198	0.036	55.7338	0.8131	-1.346	0.050
55.5420	0.1914	-1.284	0.034	55.6370	0.4993	-1.181	0.036	55.7353	0.8180	-1.332	0.049
55.5435	0.1963	-1.311	0.034	55.6385	0.5042	-1.203	0.037	55.7367	0.8225	-1.370	0.042
55.5449	0.2008	-1.313	0.033	55.6399	0.5087	-1.195	0.037	55.7382	0.8274	-1.361	0.038
55.5464	0.2057	-1.333	0.032	55.6414	0.5136	-1.189	0.038	55.7396	0.8319	-1.367	0.037
55.5478	0.2102	-1.320	0.033	55.6428	0.5181	-1.197	0.037	55.7410	0.8364	-1.384	0.042
55.5493	0.2151	-1.349	0.031	55.6443	0.5230	-1.188	0.037	55.7425	0.8413	-1.357	0.040
55.5507	0.2196	-1.319	0.033	55.6457	0.5275	-1.175	0.038	55.7439	0.8458	-1.390	0.042
55.5522	0.2245	-1.315	0.034	55.6472	0.5324	-1.181	0.038	55.7454	0.8507	-1.354	0.041
55.5536	0.2290	-1.306	0.033	55.6486	0.5369	-1.174	0.038	55.7468	0.8552	-1.331	0.042
55.5551	0.2339	-1.328	0.033	55.6501	0.5418	-1.174	0.041	55.7483	0.8601	-1.348	0.043
55.5565	0.2384	-1.340	0.033	55.6526	0.5499	-1.191	0.044	55.7497	0.8646	-1.362	0.042
55.5579	0.2429	-1.336	0.032	55.6539	0.5541	-1.154	0.057	55.7512	0.8695	-1.310	0.053
55.5594	0.2478	-1.331	0.033	55.6553	0.5586	-1.169	0.061	55.7526	0.8740	-1.315	0.044
55.5608	0.2523	-1.345	0.033	55.6566	0.5629	-1.198	0.048	55.7541	0.8789	-1.346	0.044
55.5622	0.2569	-1.338	0.033	55.6579	0.5671	-1.173	0.048	55.7555	0.8834	-1.326	0.045
55.5637	0.2617	-1.345	0.033	55.6593	0.5716	-1.183	0.046	55.7570	0.8883	-1.312	0.044
55.5651	0.2663	-1.345	0.034	55.6606	0.5758	-1.188	0.042	55.7584	0.8928	-1.320	0.042
55.5665	0.2708	-1.356	0.032	55.6619	0.5800	-1.184	0.041	55.7599	0.8977	-1.326	0.042
55.5680	0.2757	-1.356	0.033	55.6632	0.5843	-1.176	0.041	55.7613	0.9022	-1.314	0.044
55.5694	0.2802	-1.352	0.033	55.6667	0.5956	-1.168	0.041	55.7627	0.9068	-1.305	0.040
55.5709	0.2851	-1.347	0.033	55.6681	0.6001	-1.182	0.038	55.7642	0.9116	-1.319	0.042
55.5723	0.2896	-1.336	0.033	55.6695	0.6047	-1.181	0.039	55.7656	0.9162	-1.307	0.048
55.5737	0.2941	-1.351	0.034	55.6710	0.6095	-1.174	0.038	55.7670	0.9207	-1.272	0.052
55.5752	0.2990	-1.334	0.034	55.6724	0.6141	-1.188	0.038	55.7685	0.9256	-1.291	0.054
55.5766	0.3035	-1.347	0.034	55.6738	0.6186	-1.183	0.038	55.7699	0.9301	-1.296	0.045
55.5780	0.3081	-1.346	0.033	55.6753	0.6235	-1.208	0.039	55.7713	0.9346	-1.290	0.043
55.5795	0.3129	-1.329	0.033	55.6767	0.6280	-1.184	0.040	55.7728	0.9395	-1.253	0.048
55.5809	0.3175	-1.334	0.033	55.6781	0.6325	-1.193	0.044	55.7742	0.9440	-1.278	0.049
55.5823	0.3220	-1.334	0.034	55.6796	0.6374	-1.215	0.041	55.7757	0.9489	-1.235	0.063
55.5838	0.3269	-1.322	0.033	55.6810	0.6419	-1.255	0.043	55.7771	0.9534	-1.258	0.043
55.5852	0.3314	-1.325	0.034	55.6824	0.6465	-1.233	0.047	55.7785	0.9580	-1.239	0.045
55.5866	0.3360	-1.318	0.034	55.6839	0.6513	-1.246	0.042	55.7800	0.9628	-1.207	0.060
55.5881	0.3408	-1.342	0.034	55.6853	0.6559	-1.252	0.042	55.7814	0.9674	-1.218	0.054
55.5895	0.3454	-1.323	0.034	55.6868	0.6607	-1.264	0.044	55.7828	0.9719	-1.209	0.059
55.5910	0.3502	-1.312	0.034	55.6882	0.6653	-1.240	0.052	55.7843	0.9768	-1.184	0.062
55.5924	0.3548	-1.320	0.034	55.6896	0.6698	-1.227	0.053	55.7857	0.9813	-1.207	0.051
55.5939	0.3596	-1.326	0.039	55.6911	0.6747	-1.279	0.045	55.7871	0.9859	-1.179	0.055
55.5953	0.3642	-1.306	0.036	55.6925	0.6792	-1.285	0.045	55.7886	0.9907	-1.193	0.056
55.5968	0.3690	-1.297	0.035	55.6940	0.6841	-1.287	0.040	55.7900	0.9953	-1.168	0.058
55.5982	0.3736	-1.309	0.036	55.6954	0.6886	-1.300	0.040	55.7915	0.0001	-1.123	0.069
55.5996	0.3781	-1.313	0.034	55.6969	0.6935	-1.306	0.041				
55.6011	0.3830	-1.292	0.033	55.6983	0.6980	-1.326	0.042				

**Table A6.** The original data of V53 in  $R$  band observed by 2.15-m telescope at CASLEO. Hel. JD 245 5300+.

Hel. JD	Phase	$\Delta m$	Errors	Hel. JD	Phase	$\Delta m$	Errors	Hel. JD	Phase	$\Delta m$	Errors
52.6230	0.7299	-1.023	0.041	52.7557	0.1600	-0.969	0.049	52.8386	0.4287	-0.976	0.051
52.6241	0.7334	-1.025	0.041	52.7567	0.1632	-0.967	0.050	52.8397	0.4323	-0.958	0.054
52.6252	0.7370	-1.015	0.043	52.7578	0.1668	-0.960	0.052	52.8408	0.4358	-0.974	0.051
52.6263	0.7406	-1.027	0.041	52.7589	0.1704	-0.937	0.061	52.8419	0.4394	-0.966	0.056
52.6328	0.7616	-1.047	0.042	52.7600	0.1739	-0.974	0.047	53.6632	0.1015	-0.902	0.046
52.6339	0.7652	-1.049	0.041	52.7611	0.1775	-0.963	0.051	53.6643	0.1051	-0.894	0.047
52.6350	0.7688	-1.033	0.042	52.7622	0.1811	-0.975	0.048	53.6653	0.1083	-0.901	0.046
52.6361	0.7723	-1.049	0.042	52.7633	0.1846	-0.978	0.047	53.6664	0.1119	-0.891	0.046
52.6372	0.7759	-1.039	0.042	52.7644	0.1882	-0.978	0.052	53.6675	0.1155	-0.898	0.050
52.6383	0.7795	-1.058	0.040	52.7655	0.1918	-0.989	0.046	53.6686	0.1190	-0.900	0.046
52.6553	0.8346	-1.038	0.044	52.7666	0.1953	-0.971	0.053	53.6732	0.1339	-0.911	0.049
52.6564	0.8381	-1.027	0.043	52.7677	0.1989	-0.995	0.047	53.6743	0.1375	-0.927	0.056
52.6575	0.8417	-1.051	0.042	52.7688	0.2025	-1.004	0.047	53.6754	0.1411	-0.923	0.047
52.6586	0.8453	-1.053	0.043	52.7699	0.2060	-0.988	0.053	53.6801	0.1563	-0.934	0.055
52.6597	0.8488	-1.052	0.042	52.7710	0.2096	-0.990	0.058	53.6811	0.1595	-0.944	0.056
52.6706	0.8842	-1.033	0.042	52.7721	0.2132	-0.987	0.078	53.6822	0.1631	-0.965	0.044
52.6717	0.8877	-1.032	0.044	52.7732	0.2167	-1.004	0.069	53.6868	0.1780	-0.972	0.051
52.6727	0.8910	-1.030	0.041	52.7743	0.2203	-0.983	0.065	53.6879	0.1816	-0.974	0.049
52.6738	0.8945	-1.026	0.042	52.7754	0.2238	-1.020	0.054	53.6890	0.1852	-0.953	0.051
52.6749	0.8981	-1.009	0.041	52.7765	0.2274	-1.007	0.055	53.6937	0.2004	-0.964	0.082
52.6825	0.9227	-0.999	0.043	52.7776	0.2310	-0.995	0.075	53.6947	0.2036	-0.970	0.066
52.6836	0.9263	-0.996	0.043	52.7787	0.2345	-1.001	0.065	53.6958	0.2072	-0.975	0.054
52.6847	0.9299	-0.993	0.042	52.7798	0.2381	-1.005	0.066	53.7019	0.2270	-1.016	0.054
52.6857	0.9331	-0.986	0.043	52.7809	0.2417	-1.018	0.066	53.7029	0.2302	-0.984	0.050
52.6868	0.9367	-0.973	0.045	52.7820	0.2452	-1.002	0.062	53.7040	0.2338	-0.991	0.054
52.6941	0.9603	-0.952	0.044	52.7831	0.2488	-1.027	0.059	53.7087	0.2490	-1.007	0.056
52.6952	0.9639	-0.957	0.045	52.7842	0.2524	-1.036	0.059	53.7097	0.2523	-1.008	0.052
52.6963	0.9675	-0.946	0.046	52.7874	0.2627	-1.035	0.051	53.7108	0.2558	-1.005	0.048
52.6974	0.9710	-0.943	0.046	52.7885	0.2663	-1.019	0.058	53.7199	0.2853	-1.024	0.048
52.6985	0.9746	-0.942	0.046	52.7896	0.2699	-1.029	0.049	53.7210	0.2889	-1.025	0.044
52.7061	0.9992	-0.917	0.047	52.7907	0.2734	-1.017	0.055	53.7221	0.2924	-1.018	0.045
52.7072	0.0028	-0.904	0.046	52.7918	0.2770	-1.019	0.054	53.7233	0.2963	-1.012	0.045
52.7083	0.0064	-0.890	0.048	52.7928	0.2802	-1.043	0.054	53.7243	0.2996	-1.054	0.043
52.7094	0.0099	-0.891	0.048	52.7939	0.2838	-1.011	0.062	53.7254	0.3031	-1.042	0.043
52.7105	0.0135	-0.890	0.046	52.7950	0.2874	-1.024	0.061	53.7266	0.3070	-1.030	0.045
52.7122	0.0190	-0.893	0.047	52.7961	0.2909	-1.024	0.056	53.7276	0.3103	-1.026	0.043
52.7133	0.0226	-0.908	0.045	52.7972	0.2945	-1.013	0.053	53.7287	0.3138	-1.023	0.043
52.7144	0.0261	-0.900	0.046	52.7993	0.3013	-1.034	0.052	53.7384	0.3453	-1.020	0.044
52.7155	0.0297	-0.891	0.046	52.8004	0.3049	-1.023	0.054	53.7395	0.3488	-1.008	0.046
52.7166	0.0333	-0.893	0.048	52.8015	0.3084	-1.019	0.059	53.7406	0.3524	-1.000	0.046
52.7192	0.0417	-0.892	0.046	52.8025	0.3117	-1.023	0.048	53.7419	0.3566	-1.012	0.049
52.7203	0.0452	-0.899	0.049	52.8036	0.3153	-1.001	0.056	53.7430	0.3602	-1.010	0.051
52.7214	0.0488	-0.886	0.049	52.8047	0.3188	-1.027	0.054	53.7501	0.3832	-0.993	0.071
52.7225	0.0524	-0.906	0.047	52.8058	0.3224	-0.984	0.086	53.7511	0.3864	-1.008	0.053
52.7236	0.0559	-0.897	0.046	52.8069	0.3259	-1.011	0.066	53.7522	0.3900	-0.979	0.051
52.7247	0.0595	-0.899	0.046	52.8080	0.3295	-0.993	0.062	53.7533	0.3936	-0.989	0.059
52.7258	0.0631	-0.900	0.046	52.8091	0.3331	-1.025	0.074	53.7543	0.3968	-0.985	0.055
52.7269	0.0666	-0.903	0.045	52.8102	0.3366	-1.000	0.061	53.7654	0.4328	-0.979	0.064
52.7280	0.0702	-0.909	0.046	52.8112	0.3399	-1.024	0.056	53.7665	0.4364	-0.931	0.068
52.7290	0.0734	-0.912	0.046	52.8123	0.3435	-1.023	0.065	53.7676	0.4399	-0.936	0.079
52.7301	0.0770	-0.911	0.046	52.8134	0.3470	-1.019	0.060	53.7686	0.4432	-0.960	0.073
52.7312	0.0806	-0.900	0.046	52.8145	0.3506	-1.020	0.057	53.7746	0.4626	-0.929	0.051
52.7323	0.0841	-0.908	0.047	52.8156	0.3541	-1.018	0.051	53.7756	0.4659	-0.944	0.053
52.7334	0.0877	-0.898	0.047	52.8167	0.3577	-1.015	0.049	53.7767	0.4694	-0.917	0.053
52.7345	0.0913	-0.894	0.046	52.8178	0.3613	-0.998	0.062	53.7777	0.4727	-0.924	0.065
52.7356	0.0948	-0.889	0.046	52.8189	0.3648	-1.009	0.053	53.7788	0.4762	-0.926	0.054
52.7367	0.0984	-0.897	0.048	52.8199	0.3681	-1.008	0.049	53.7874	0.5041	-0.884	0.057
52.7377	0.1016	-0.919	0.046	52.8210	0.3717	-0.999	0.052	53.7884	0.5073	-0.888	0.055
52.7388	0.1052	-0.909	0.045	52.8221	0.3752	-0.992	0.057	53.7895	0.5109	-0.901	0.056
52.7399	0.1088	-0.901	0.047	52.8232	0.3788	-1.013	0.055	53.7955	0.5304	-0.891	0.071
52.7415	0.1140	-0.911	0.047	52.8243	0.3823	-0.996	0.051	53.7965	0.5336	-0.873	0.074

**Table A6 – continued**

Hel. JD	Phase	$\Delta m$	Errors	Hel. JD	Phase	$\Delta m$	Errors	Hel. JD	Phase	$\Delta m$	Errors
52.7426	0.1175	-0.906	0.048	52.8254	0.3859	-1.021	0.046	53.8044	0.5592	-0.893	0.084
52.7437	0.1211	-0.917	0.046	52.8265	0.3895	-0.996	0.045	53.8160	0.5968	-0.892	0.089
52.7448	0.1247	-0.928	0.047	52.8276	0.3930	-1.009	0.047	53.8269	0.6321	-0.917	0.078
52.7459	0.1282	-0.915	0.051	52.8287	0.3966	-1.014	0.047	53.8279	0.6354	-0.928	0.073
52.7469	0.1315	-0.917	0.048	52.8298	0.4002	-0.987	0.051	53.8290	0.6389	-0.926	0.063
52.7480	0.1350	-0.914	0.051	52.8309	0.4037	-1.022	0.046	53.8301	0.6425	-0.938	0.064
52.7491	0.1386	-0.928	0.048	52.8320	0.4073	-1.008	0.044	53.8311	0.6458	-0.948	0.070
52.7502	0.1422	-0.928	0.052	52.8331	0.4109	-1.010	0.046	53.8351	0.6587	-0.895	0.113
52.7513	0.1457	-0.942	0.049	52.8342	0.4144	-1.006	0.045	53.8361	0.6620	-0.929	0.088
52.7524	0.1493	-0.948	0.048	52.8353	0.4180	-0.989	0.047	53.8372	0.6655	-0.967	0.072
52.7535	0.1529	-0.945	0.050	52.8364	0.4216	-0.998	0.048	53.8393	0.6723	-0.986	0.073
52.7546	0.1564	-0.961	0.049	52.8375	0.4251	-0.987	0.050				

**Table A7.** The original data of V53 in  $I$  band observed by 2.15-m telescope at CASLEO. Hel. JD 245 5300+.

Hel. JD	Phase	$\Delta m$	Errors	Hel. JD	Phase	$\Delta m$	Errors	Hel. JD	Phase	$\Delta m$	Errors
52.6402	0.7856	-0.924	0.046	53.5704	0.8007	-0.919	0.048	53.6512	0.0626	-0.755	0.053
52.6413	0.7892	-0.921	0.044	53.5714	0.8040	-0.907	0.048	53.6523	0.0662	-0.768	0.052
52.6424	0.7927	-0.934	0.045	53.5725	0.8075	-0.913	0.050	53.6534	0.0698	-0.768	0.052
52.6435	0.7963	-0.936	0.046	53.5736	0.8111	-0.905	0.051	53.6544	0.0730	-0.755	0.054
52.6446	0.7999	-0.919	0.046	53.5746	0.8143	-0.920	0.048	53.6559	0.0779	-0.768	0.052
52.6457	0.8034	-0.928	0.046	53.5757	0.8179	-0.915	0.048	53.6569	0.0811	-0.770	0.052
52.6468	0.8070	-0.929	0.046	53.5768	0.8215	-0.898	0.047	53.6580	0.0847	-0.762	0.054
52.6479	0.8106	-0.917	0.046	53.5778	0.8247	-0.917	0.047	53.6591	0.0882	-0.789	0.054
52.6490	0.8141	-0.941	0.046	53.5789	0.8283	-0.929	0.046	53.6601	0.0915	-0.781	0.052
52.6501	0.8177	-0.928	0.046	53.5799	0.8315	-0.931	0.046	53.6612	0.0950	-0.765	0.052
52.6626	0.8582	-0.921	0.047	53.5810	0.8351	-0.929	0.045	53.6699	0.1232	-0.773	0.052
52.6637	0.8618	-0.918	0.046	53.5821	0.8387	-0.926	0.048	53.6709	0.1265	-0.777	0.052
52.6648	0.8654	-0.921	0.046	53.5831	0.8419	-0.907	0.047	53.6720	0.1301	-0.808	0.051
52.6659	0.8689	-0.912	0.047	53.5842	0.8455	-0.924	0.050	53.6767	0.1453	-0.807	0.054
52.6670	0.8725	-0.910	0.047	53.5853	0.8490	-0.918	0.047	53.6778	0.1489	-0.805	0.054
52.6767	0.9039	-0.887	0.047	53.5863	0.8523	-0.922	0.046	53.6788	0.1521	-0.820	0.053
52.6777	0.9072	-0.902	0.047	53.5874	0.8558	-0.899	0.049	53.6834	0.1670	-0.842	0.050
52.6788	0.9107	-0.901	0.048	53.5885	0.8594	-0.897	0.054	53.6845	0.1706	-0.841	0.054
52.6799	0.9143	-0.891	0.048	53.5895	0.8626	-0.901	0.051	53.6856	0.1741	-0.862	0.053
52.6810	0.9179	-0.892	0.048	53.5906	0.8662	-0.917	0.047	53.6903	0.1894	-0.863	0.053
52.6882	0.9412	-0.862	0.048	53.5917	0.8698	-0.911	0.047	53.6914	0.1929	-0.866	0.050
52.6892	0.9444	-0.876	0.048	53.5927	0.8730	-0.925	0.048	53.6924	0.1962	-0.870	0.051
52.6903	0.9480	-0.875	0.049	53.5938	0.8766	-0.903	0.050	53.6971	0.2114	-0.873	0.062
52.6914	0.9516	-0.856	0.049	53.5949	0.8801	-0.907	0.046	53.6982	0.2150	-0.879	0.056
52.6925	0.9551	-0.853	0.049	53.5959	0.8834	-0.909	0.046	53.6993	0.2185	-0.871	0.067
52.7000	0.9794	-0.819	0.052	53.5970	0.8869	-0.905	0.046	53.7053	0.2380	-0.890	0.063
52.7011	0.9830	-0.793	0.055	53.5981	0.8905	-0.897	0.048	53.7063	0.2412	-0.877	0.063
52.7022	0.9866	-0.806	0.051	53.6013	0.9009	-0.883	0.047	53.7074	0.2448	-0.890	0.060
52.7033	0.9901	-0.795	0.052	53.6024	0.9045	-0.913	0.048	53.7121	0.2600	-0.910	0.050
52.7044	0.9937	-0.802	0.052	53.6035	0.9080	-0.881	0.048	53.7132	0.2636	-0.909	0.050
53.5239	0.6500	-0.828	0.052	53.6046	0.9116	-0.881	0.047	53.7143	0.2672	-0.912	0.052
53.5249	0.6532	-0.816	0.052	53.6056	0.9148	-0.867	0.047	53.7164	0.2740	-0.908	0.049
53.5260	0.6568	-0.802	0.053	53.6067	0.9184	-0.868	0.047	53.7174	0.2772	-0.918	0.051
53.5270	0.6601	-0.822	0.058	53.6078	0.9220	-0.879	0.050	53.7185	0.2808	-0.921	0.051
53.5281	0.6636	-0.846	0.063	53.6089	0.9255	-0.866	0.048	53.7315	0.3229	-0.918	0.047
53.5292	0.6672	-0.836	0.057	53.6099	0.9288	-0.870	0.048	53.7325	0.3262	-0.930	0.048
53.5302	0.6704	-0.821	0.068	53.6110	0.9323	-0.855	0.049	53.7336	0.3297	-0.921	0.048
53.5313	0.6740	-0.845	0.060	53.6128	0.9382	-0.841	0.048	53.7347	0.3333	-0.929	0.048
53.5324	0.6776	-0.829	0.051	53.6139	0.9417	-0.841	0.049	53.7358	0.3369	-0.926	0.049
53.5334	0.6808	-0.842	0.060	53.6149	0.9450	-0.834	0.052	53.7369	0.3404	-0.925	0.049
53.5345	0.6844	-0.861	0.050	53.6160	0.9485	-0.849	0.051	53.7445	0.3651	-0.890	0.049
53.5356	0.6879	-0.848	0.052	53.6171	0.9521	-0.825	0.050	53.7456	0.3686	-0.889	0.053
53.5367	0.6915	-0.871	0.051	53.6182	0.9557	-0.819	0.052	53.7467	0.3722	-0.890	0.050

**Table A7 – continued**

Hel. JD	Phase	$\Delta m$	Errors	Hel. JD	Phase	$\Delta m$	Errors	Hel. JD	Phase	$\Delta m$	Errors
53.5377	0.6947	-0.844	0.056	53.6192	0.9589	-0.831	0.049	53.7477	0.3754	-0.893	0.056
53.5388	0.6983	-0.852	0.050	53.6203	0.9625	-0.821	0.052	53.7488	0.3790	-0.906	0.067
53.5399	0.7019	-0.858	0.059	53.6214	0.9660	-0.828	0.050	53.7595	0.4137	-0.870	0.059
53.5410	0.7054	-0.865	0.054	53.6224	0.9693	-0.821	0.050	53.7606	0.4172	-0.886	0.058
53.5420	0.7087	-0.867	0.050	53.6235	0.9728	-0.824	0.050	53.7616	0.4205	-0.887	0.060
53.5431	0.7122	-0.866	0.050	53.6246	0.9764	-0.807	0.056	53.7627	0.4240	-0.855	0.058
53.5442	0.7158	-0.862	0.053	53.6257	0.9800	-0.808	0.050	53.7638	0.4276	-0.881	0.056
53.5454	0.7197	-0.859	0.057	53.6267	0.9832	-0.791	0.053	53.7699	0.4474	-0.853	0.073
53.5465	0.7233	-0.881	0.057	53.6278	0.9868	-0.772	0.051	53.7710	0.4509	-0.838	0.057
53.5476	0.7268	-0.869	0.053	53.6289	0.9903	-0.773	0.053	53.7721	0.4545	-0.859	0.066
53.5486	0.7301	-0.868	0.057	53.6299	0.9936	-0.797	0.054	53.7731	0.4578	-0.798	0.071
53.5497	0.7336	-0.888	0.048	53.6310	0.9972	-0.776	0.051	53.7817	0.4856	-0.816	0.061
53.5508	0.7372	-0.886	0.050	53.6321	0.0007	-0.783	0.052	53.7827	0.4889	-0.820	0.060
53.5518	0.7404	-0.885	0.048	53.6331	0.0040	-0.765	0.054	53.7838	0.4924	-0.806	0.066
53.5529	0.7440	-0.914	0.046	53.6342	0.0075	-0.803	0.054	53.7849	0.4960	-0.800	0.066
53.5540	0.7476	-0.897	0.046	53.6352	0.0108	-0.786	0.052	53.7859	0.4992	-0.798	0.060
53.5551	0.7511	-0.905	0.050	53.6363	0.0143	-0.761	0.052	53.7919	0.5187	-0.754	0.096
53.5562	0.7547	-0.918	0.047	53.6374	0.0179	-0.777	0.052	53.7929	0.5219	-0.785	0.080
53.5572	0.7579	-0.910	0.046	53.6384	0.0211	-0.795	0.052	53.7940	0.5255	-0.789	0.067
53.5583	0.7615	-0.880	0.050	53.6395	0.0247	-0.755	0.054	53.7995	0.5433	-0.809	0.070
53.5594	0.7651	-0.875	0.053	53.6406	0.0283	-0.768	0.054	53.8006	0.5469	-0.794	0.092
53.5604	0.7683	-0.886	0.046	53.6416	0.0315	-0.751	0.055	53.8094	0.5754	-0.827	0.067
53.5615	0.7719	-0.881	0.049	53.6427	0.0351	-0.765	0.052	53.8126	0.5858	-0.808	0.086
53.5626	0.7754	-0.902	0.047	53.6438	0.0386	-0.763	0.052	53.8137	0.5894	-0.794	0.095
53.5636	0.7787	-0.898	0.048	53.6448	0.0419	-0.756	0.051	53.8213	0.6140	-0.796	0.102
53.5647	0.7823	-0.887	0.052	53.6459	0.0455	-0.762	0.052	53.8234	0.6208	-0.796	0.096
53.5658	0.7858	-0.906	0.047	53.6470	0.0490	-0.747	0.055	53.8245	0.6244	-0.801	0.102
53.5672	0.7904	-0.910	0.047	53.6480	0.0523	-0.744	0.059	53.8255	0.6276	-0.836	0.091
53.5682	0.7936	-0.906	0.048	53.6491	0.0558	-0.760	0.052				
53.5693	0.7972	-0.908	0.052	53.6502	0.0594	-0.749	0.053				

This paper has been typeset from a TeX/LaTeX file prepared by the author.